

~~CONFIDENTIAL~~
UNCLASSIFIED
NACA

RESEARCH MEMORANDUM

for the
U. S. Air Force

WIND-TUNNEL INVESTIGATION OF A MODIFIED 1/20-SCALE MODEL
OF THE CONVAIR MX-1554 AIRPLANE AT MACH NUMBERS
OF 1.41 AND 2.01

By John H. Hilton, Jr., and Edward B. Palazzo

Langley Aeronautical Laboratory
Langley Field, Va.

To UNCLASSIFIED

By authority of TPA # 63

Date 12/13/61
Effective
mag

CLASSIFIED DOCUMENT

This material contains information affecting the National Defense of the United States within the meaning of the espionage laws, Title 18, U.S.C., Secs. 793 and 794, the transmission or revelation of which in any manner to an unauthorized person is prohibited by law.

NATIONAL ADVISORY COMMITTEE FOR AERONAUTICS

WASHINGTON

AUG 24 1953

UNCLASSIFIED

~~CONFIDENTIAL~~



3 1176 01438 6081

NATIONAL ADVISORY COMMITTEE FOR AERONAUTICS

RESEARCH MEMORANDUM

for the

U. S. Air Force

WIND-TUNNEL INVESTIGATION OF A MODIFIED 1/20-SCALE MODEL

OF THE CONVAIR MX-1554 AIRPLANE AT MACH NUMBERS

OF 1.41 AND 2.01

By John H. Hilton, Jr., and Edward B. Palazzo

SUMMARY

An investigation of a 1/20-scale model of the Convair MX-1554 airplane has been conducted in the Langley 4- by 4-foot supersonic pressure tunnel to evaluate the effects of extending the length of the fuselage afterbody (in accordance with area-rule considerations) and to provide longitudinal and lateral stability and control data. The tests were made at Mach numbers of 1.41 and 2.01 over a Reynolds number range of 1.13×10^6 to 8.83×10^6 .

The results of the tests indicate that extension of the fuselage afterbody length caused little change in the minimum longitudinal force coefficient and in the drag due to lift. Elongating the afterbody resulted in slight increases in the static longitudinal stability, static directional stability, and side force and had negligible effect on the other parameters.

The variation of trim lift coefficient with elevon deflection for the basic configuration decreased from -0.011 at $M = 1.41$ to -0.007 at $M = 2.01$.

The data indicated a value of -0.3 for $\left(\beta_{\delta_R}\right)_{C_n=0}$ at $M = 1.41$,

$\alpha = 4^\circ$. The directional stability of the basic configuration decreases with increasing Mach number and is approaching zero near $M = 2.0$, $\alpha = 4^\circ$.

Reynolds number effects were small; however, some increase in $\Delta C_D / C_L^2$ was indicated at low Reynolds numbers for both test Mach numbers.

UNCLASSIFIED

INTRODUCTION

An investigation has been conducted in the Langley 4- by 4-foot supersonic pressure tunnel to determine the aerodynamic characteristics of the Convair MX-1554 aircraft configuration. The present tests of the MX-1554 constitute the second phase of a specific research project conducted at the request of the United States Air Force. The results of the first phase of this research project (presented in ref. 1) were concerned with the aerodynamic characteristics of the configuration at Mach numbers of 1.61 and 2.01. The present tests were conducted at $M = 1.41$ and $M = 2.01$ to provide additional data for the MX-1554 design and to determine the effects of extending the length of the fuselage afterbody. The changes in the afterbody shape were proposed (on the basis of Langley 8-foot transonic tunnel tests) as a means of reducing the transonic minimum drag rise and were dictated by the area-rule concept. The basic model (short afterbody) of the present tests had a different nose and a different canopy compared to the Phase I configuration (ref. 1).

COEFFICIENTS AND SYMBOLS

The data are referred to the stability-axes system (fig. 1) with the reference center of gravity at 27.5 percent of the wing mean aerodynamic chord.

The coefficients and symbols are defined as follows:

C_L	lift coefficient, $-Z/qS$
C_X	longitudinal-force coefficient, X/qS
C_D	drag coefficient, $\frac{\text{Drag}}{qS}$
$C_{D_{\min}}$	minimum drag coefficient
$\Delta C_D = C_D - C_{D_{\min}}$	
C_m	pitching-moment coefficient, $M'/qS\bar{c}$
C_Y	lateral-force coefficient, Y/qS
C_n	yawing-moment coefficient, N/qSb

C_L	rolling-moment coefficient, L/qSb
X	force along X-axis, lb
Y	force along Y-axis, lb
Z	force along Z-axis, lb
L	moment about X-axis, lb-ft
M'	moment about Y-axis, lb-ft
N	moment about Z-axis, lb-ft
q	free-stream dynamic pressure, lb/sq ft
R	Reynolds number
S	total wing area, sq ft
b	wing span, ft
\bar{c}	wing mean aerodynamic chord, ft
c	local wing chord, ft
M	Mach number
p_o	tunnel stagnation pressure, lb/sq in
α	angle of attack of fuselage center line, deg
β	angle of sideslip, deg
δ_e	elevon deflection angle, deg
δ_R	rudder deflection angle, deg
C_{L_α}	lift-curve slope
C_{mC_L}	longitudinal-stability parameter, rate of change of pitching-moment coefficient with lift coefficient, $\partial C_m / \partial C_L$

$C_{n\beta}$	directional-stability parameter, rate of change of yawing-moment coefficient with angle of sideslip, $\partial C_n / \partial \beta$
$C_{l\beta}$	effective-dihedral parameter, rate of change of rolling-moment coefficient with angle of sideslip, $\partial C_l / \partial \beta$
$C_{Y\beta}$	lateral-force parameter, rate of change of lateral-force coefficient with angle of sideslip, $\partial C_Y / \partial \beta$
$(C_{L\delta_e})_{\text{trim}}$	rate of change of lift coefficient with elevon deflection at $C_m = 0$, $\partial C_L / \partial \delta_e$
$(\alpha_{\delta_e})_{\text{trim}}$	rate of change of angle of attack with elevon deflection at $C_m = 0$, $\partial \alpha / \partial \delta_e$
$(\beta_{\delta_R})_{C_n = 0}$	rate of change of angle of sideslip with rudder deflection at $C_n = 0$, $\partial \beta / \partial \delta_R$

Configuration symbols:

W	wing
B	body
C_1	blunt-canopy, inclined 30°
C_7	vee-canopy
P	nose probe
N_3	blunt, interim nose shape
N_4	pointed, final nose shape
VT_{60}	vertical tail, 60° sweptback leading edge, 5° swept-forward trailing edge
VT_{60-1}	vertical tail, 60° sweptback leading edge, 0° swept-forward trailing edge
D_0	inlets open

D_F	inlets closed with faired plugs
D_F^O	inlets open and closed
F	chordwise wing fences on
F_W^O	chordwise wing fences both on and off

MODEL AND APPARATUS

The tests were conducted in the Langley 4- by 4-foot supersonic pressure tunnel at $M = 1.41$ and 2.01 .

The 1/20-scale model of the Convair MX-1554 airplane used in this investigation is shown in figure 2. Details of the model (which was supplied by the contractor) are given in table I. The basic configuration for the present (designated herein as Phase II) tests had a 60° delta wing mounted on the short fuselage in a mid-low position and had NACA 0004-65 (mod.) airfoil sections. The vertical tail was similar in plan form and section to the wing semispan. The model was equipped with wing trailing-edge flaps and a rudder. The configuration had chordwise wing fences and a probe projecting from the nose. Twin ram-type inlets were located well forward on the sides of the fuselage, but for the present tests (Phase II) the inlets were closed by means of faired plugs. The blunt interim nose N_3 and the blunt 30° optical flat canopy C_1 tested as part of the Phase I basic configuration were replaced by a pointed nose shape N_4 and a sharp-leading-edge vee-canopy C_7 for the Phase II tests.

Three different afterbodies (fig. 3) were tested: a short symmetrical afterbody (which was part of the basic configuration); an elongated symmetrical afterbody; and an elongated upswept afterbody, designed to provide ground clearance. The latter two afterbodies, which have base areas approximately the same as the base area of the short symmetrical afterbody, were designed to provide a more gradual decrease in the cross-sectional area distribution of the complete configuration. Figure 4 presents a series of photographs showing the complete configuration with the different afterbodies installed. The cross-sectional area distribution of the complete model with the various afterbodies is given in figure 5.

A body of revolution (fig. 6) having the same cross-sectional area distribution as the complete basic configuration ($WBPFN_4C_7VT_{60}D_F$ + Short symmetrical afterbody) was tested to provide additional data for area-rule consideration.

Forces and moments were measured by means of a six-component internal strain-gage balance and indicating system.

TESTS

The model was mounted on a 4° bent sting which enabled pitch tests to be made through an angle-of-attack range from -4° to 12° at $\beta = 0^\circ$ and sideslip tests to be conducted through a range of sideslip angles from -4° to 12° at 0° and 4° angle of attack.

The various conditions for the tests were:

Mach number	Reynolds number, based on M.A.C.	Stagnation pressure, lb/sq in. abs.	Stagnation temperature, $^\circ\text{F}$
1.41	1.37×10^6	4	100
	3.08	9	100
	4.80	14	100
	7.02	21	110
	8.83	27	120
2.01	1.13	4*	100
	2.55	9	100
	3.96	14	100
	5.83	21	108
	7.27	27	120

*For this low stagnation pressure, the test section Mach number was approximately 1.97.

The stagnation dew point for the test was less than -25°F .

CORRECTIONS AND ACCURACY

The angles of attack and sideslip have been corrected for deflections of the balance and sting caused by the aerodynamic loads and are estimated to be accurate within $\pm 0.2^\circ$. The estimated accuracy of the control-deflection settings was $\pm 0.1^\circ$.

No corrections were made for Mach number gradient and flow angularity. It should be noted that center-line calibration measurements of the $M = 2.0$ nozzle indicate that the free-stream Mach number drops to 1.97 at $p_0 = 4$ lb/sq in. abs. Accordingly, the low Reynolds number data

have been computed for a free-stream $M = 1.97$. Inasmuch as this change in M is small, the data are presented on the $M = 2.01$ plots. The variations of Mach number and flow angularity are:

	$M = 1.41$	$M = 2.01$	
	p_o , lb/sq in. abs.	p_o , lb/sq in. abs.	
	4, 9, 14, 21, 27	4	9, 14, 21, 27
Mach number variation in nozzle	± 0.01	1.97 ± 0.015	± 0.01
Air-stream angularity in horizontal plane, deg	+0.0 -0.25	± 0.05	± 0.05
Air-stream angularity in vertical plane, deg	+0.15 -0.25	± 0.1	± 0.05

The estimated errors in the coefficients are as follows:

C_L	± 0.005
C_X	± 0.001
C_m	± 0.002
C_Y	± 0.003
C_n	± 0.0002
C_l	± 0.0002

Base-pressure measurements were made for all tests and the longitudinal-force coefficients were corrected to correspond to a base pressure equal to free-stream static pressure. It is believed that sting interference effects on the upswept afterbody are small and that the changes in the upswept afterbody (fig. 3) to provide sting clearance had little effect on the aerodynamic characteristics.

PRESENTATION OF RESULTS

The results of the investigation are presented in figures 7 to 16 as follows:

Data presentedLongitudinal characteristicsFigure

Pitch tests, with various elevon deflections, of the complete configuration with the short symmetrical afterbody, the elongated symmetrical afterbody, and the elongated unswept afterbody.

7

- (a) $M = 1.41$; $R = 4.80 \times 10^6$
(b) $M = 2.01$; $R = 3.96 \times 10^6$

Pitch tests of the complete basic configuration (short symmetrical afterbody) at various Reynolds numbers.

8

- (a) $M = 1.41$
(b) $M = 2.01$

Curves of ΔC_D versus C_L^2 for the various test configurations at $M = 1.41$ and 2.01 , $\delta_e = 0^\circ$. Variable R data are presented for the basic configuration.

9

Pitch tests of the complete basic configuration (short symmetrical afterbody), the wing-body combination, and the "equivalent-area" distribution body of revolution. $M = 1.41$; $R = 4.8 \times 10^6$.

10

Lateral characteristics

Sideslip tests at $\alpha = 0^\circ$ of the complete basic configuration (short symmetrical afterbody) with and without the vertical tail.

11

- (a) $M = 1.41$; $R = 4.80 \times 10^6$
(b) $M = 2.01$; $R = 3.96 \times 10^6$

Sideslip tests at $\alpha = 4^\circ$, $\delta_R = 0^\circ$, of the complete configuration with the short symmetrical afterbody, the elongated symmetrical afterbody, and the elongated upswept afterbody.

12

Sideslip test at $\alpha = 4^\circ$, $\delta_R = -15^\circ$, of the complete configuration with the short symmetrical afterbody.

- (a) $M = 1.41$; $R = 4.80 \times 10^6$
(b) $M = 2.01$; $R = 3.96 \times 10^6$

Sideslip tests at $\alpha = 4^\circ$ of the complete basic configuration (short symmetrical afterbody) over a Reynolds number range of 1.13×10^6 to 7.27×10^6 . $\delta_R = 0^\circ$; $M = 2.01$. 13

Variation with Mach number

Longitudinal parameters through the supersonic Mach number range. $\beta = 0^\circ$. 14

Longitudinal control parameters through the supersonic Mach number range. $\beta = 0^\circ$. 15

Lateral parameters through the supersonic Mach number range. 16

(a) $\alpha = 0^\circ$

(b) $\alpha = 4^\circ$

The longitudinal parameters $C_{L\alpha}$, C_{mC_L} , C_{Dmin} , $(C_{m\delta_e})_{\alpha=0^\circ}$, $(C_{L\delta_e})_{trim}$, and $(\alpha\delta_e)_{trim}$ are presented in table II and the lateral parameters $C_{Y\beta}$, $C_{l\beta}$, $C_{n\beta}$, and $(\beta\delta_R)_{C_n=0}$ are given in table III. Table IV is a compilation of the values of C_L , C_m , C_X , C_Y , C_l , and C_n measured for the various test configurations and conditions.

DISCUSSION

Longitudinal Characteristics

Basic.— Changing the nose and canopy shapes of the basic configurations from those of reference 1 had little effect on the aerodynamic characteristics; however, some reduction in drag was noted.

Afterbody extensions.— Extending the afterbody length of the complete configuration (fig. 7) caused little change in the minimum longitudinal-force coefficient and in the lift-curve slope at both test Mach numbers. The static margin of the extended afterbody configurations was approximately 0.01 higher than the values of C_{mC_L} for the basic configuration at $M = 1.41$ and 2.01 . The drag due to lift (fig. 9) showed little or no change with afterbody extension at both test Mach numbers.

Reynolds number effects.— The basic configuration was tested over a range of Reynolds numbers at $M = 1.41$ and 2.01 (figs. 8 and 9). Except for a small increase in the drag due to lift at the lowest Reynolds numbers, the Reynolds number effects were negligible. Values of $1/C_{L\alpha}$ (at the higher Reynolds numbers) are higher than $\Delta C_D/C_L^2$ at $M = 1.41$ and about the same as $\Delta C_D/C_L^2$ at $M = 2.01$. (See ref. 4 for further discussion of these data.)

Controls.— Extending the afterbody length improved the elevon effectiveness at $M = 1.41$ but had no effect on $C_{m\delta_e}$ at $M = 2.01$ (table II). The variation of the trim lift coefficient with elevon deflection for the basic configuration was -0.011 and -0.007 at $M = 1.41$ and 2.01 , respectively. The corresponding values of $(\alpha_{\delta_e})_{trim}$ were -0.34 and -0.29 . Deflection of the elevons -10° increased $C_{x_{min}}$ from -0.022 to -0.028 at $M = 1.41$ and from -0.020 to -0.023 at $M = 2.01$; the trim drag coefficient for $\delta_e = -10^\circ$ (fig. 7) was 0.032 at $M = 1.41$ and 0.024 at $M = 2.01$.

Lateral Characteristics

Basic.— The lateral characteristics of the basic configuration were only slightly affected by changing the angle of attack from 0° to 4° (figs. 11 and 12) except at $M = 1.41$, where C_{l_β} increased from -0.0006 to -0.0012 . At 4° angle of attack, $M = 2.01$, the changes in the lateral parameters were negligible as the Reynolds number was increased above the nominal test value of 3.96×10^6 (fig. 13). A small decrease in C_{Y_β} and C_{n_β} was indicated at $R = 1.13 \times 10^6$.

Afterbody extensions.— The effects of the different afterbodies on the lateral characteristics of the complete model at $\alpha = 4^\circ$ are presented in figure 12 for $M = 1.41$ and 2.01 . Increasing the afterbody length improved the directional stability and increased C_{Y_β} for the complete configuration at both test Mach numbers without affecting C_{l_β} in the range $-4^\circ < \beta < +4^\circ$. The parameters C_{n_β} , C_{Y_β} , and C_{l_β} decreased with increasing Mach number for all configurations (table III).

Controls.— Rudder deflections at $\alpha = 4^\circ$ ($M = 1.41$ and 2.01) caused little change in C_{Y_β} , C_{l_β} , and C_{n_β} (fig. 12). A value

~~CONFIDENTIAL~~
UNCLASSIFIED
NACA

RESEARCH MEMORANDUM

for the
U. S. Air Force

WIND-TUNNEL INVESTIGATION OF A MODIFIED 1/20-SCALE MODEL
OF THE CONVAIR MX-1554 AIRPLANE AT MACH NUMBERS
OF 1.41 AND 2.01

By John H. Hilton, Jr., and Edward B. Palazzo

Langley Aeronautical Laboratory
Langley Field, Va.

To UNCLASSIFIED

By authority of TPA # 63

Date 12/13/61

CLASSIFIED DOCUMENT

This material contains information affecting the National Defense of the United States within the meaning of the espionage laws, Title 18, U.S.C., Secs. 793 and 794, the transmission or revelation of which in any manner to an unauthorized person is prohibited by law.

NATIONAL ADVISORY COMMITTEE
FOR AERONAUTICS

WASHINGTON

AUG 24 1953

UNCLASSIFIED

~~CONFIDENTIAL~~



3 1176 01438 6081

NATIONAL ADVISORY COMMITTEE FOR AERONAUTICS

RESEARCH MEMORANDUM

for the

U. S. Air Force

WIND-TUNNEL INVESTIGATION OF A MODIFIED 1/20-SCALE MODEL

OF THE CONVAIR MX-1554 AIRPLANE AT MACH NUMBERS

OF 1.41 AND 2.01

By John H. Hilton, Jr., and Edward B. Palazzo

SUMMARY

An investigation of a 1/20-scale model of the Convair MX-1554 airplane has been conducted in the Langley 4- by 4-foot supersonic pressure tunnel to evaluate the effects of extending the length of the fuselage afterbody (in accordance with area-rule considerations) and to provide longitudinal and lateral stability and control data. The tests were made at Mach numbers of 1.41 and 2.01 over a Reynolds number range of 1.13×10^6 to 8.83×10^6 .

The results of the tests indicate that extension of the fuselage afterbody length caused little change in the minimum longitudinal force coefficient and in the drag due to lift. Elongating the afterbody resulted in slight increases in the static longitudinal stability, static directional stability, and side force and had negligible effect on the other parameters.

The variation of trim lift coefficient with elevon deflection for the basic configuration decreased from -0.011 at $M = 1.41$ to -0.007 at $M = 2.01$.

The data indicated a value of -0.3 for $\left(\beta_{\delta_R}\right)_{C_n=0}$ at $M = 1.41$,

$\alpha = 4^\circ$. The directional stability of the basic configuration decreases with increasing Mach number and is approaching zero near $M = 2.0$, $\alpha = 4^\circ$.

Reynolds number effects were small; however, some increase in $\Delta C_D / C_L^2$ was indicated at low Reynolds numbers for both test Mach numbers.

UNCLASSIFIED

INTRODUCTION

An investigation has been conducted in the Langley 4- by 4-foot supersonic pressure tunnel to determine the aerodynamic characteristics of the Convair MX-1554 aircraft configuration. The present tests of the MX-1554 constitute the second phase of a specific research project conducted at the request of the United States Air Force. The results of the first phase of this research project (presented in ref. 1) were concerned with the aerodynamic characteristics of the configuration at Mach numbers of 1.61 and 2.01. The present tests were conducted at $M = 1.41$ and $M = 2.01$ to provide additional data for the MX-1554 design and to determine the effects of extending the length of the fuselage afterbody. The changes in the afterbody shape were proposed (on the basis of Langley 8-foot transonic tunnel tests) as a means of reducing the transonic minimum drag rise and were dictated by the area-rule concept. The basic model (short afterbody) of the present tests had a different nose and a different canopy compared to the Phase I configuration (ref. 1).

COEFFICIENTS AND SYMBOLS

The data are referred to the stability-axes system (fig. 1) with the reference center of gravity at 27.5 percent of the wing mean aerodynamic chord.

The coefficients and symbols are defined as follows:

C_L	lift coefficient, $-Z/qS$
C_X	longitudinal-force coefficient, X/qS
C_D	drag coefficient, $\frac{\text{Drag}}{qS}$
$C_{D_{\min}}$	minimum drag coefficient
$\Delta C_D = C_D - C_{D_{\min}}$	
C_m	pitching-moment coefficient, $M'/qS\bar{c}$
C_Y	lateral-force coefficient, Y/qS
C_n	yawing-moment coefficient, N/qSb

C_L	rolling-moment coefficient, L/qSb
X	force along X-axis, lb
Y	force along Y-axis, lb
Z	force along Z-axis, lb
L	moment about X-axis, lb-ft
M'	moment about Y-axis, lb-ft
N	moment about Z-axis, lb-ft
q	free-stream dynamic pressure, lb/sq ft
R	Reynolds number
S	total wing area, sq ft
b	wing span, ft
\bar{c}	wing mean aerodynamic chord, ft
c	local wing chord, ft
M	Mach number
p_o	tunnel stagnation pressure, lb/sq in
α	angle of attack of fuselage center line, deg
β	angle of sideslip, deg
δ_e	elevon deflection angle, deg
δ_R	rudder deflection angle, deg
C_{L_α}	lift-curve slope
C_{mC_L}	longitudinal-stability parameter, rate of change of pitching-moment coefficient with lift coefficient, $\partial C_m / \partial C_L$

$C_{n\beta}$	directional-stability parameter, rate of change of yawing-moment coefficient with angle of sideslip, $\partial C_n / \partial \beta$
$C_{l\beta}$	effective-dihedral parameter, rate of change of rolling-moment coefficient with angle of sideslip, $\partial C_l / \partial \beta$
$C_{Y\beta}$	lateral-force parameter, rate of change of lateral-force coefficient with angle of sideslip, $\partial C_Y / \partial \beta$
$(C_{L\delta_e})_{\text{trim}}$	rate of change of lift coefficient with elevon deflection at $C_m = 0$, $\partial C_L / \partial \delta_e$
$(\alpha_{\delta_e})_{\text{trim}}$	rate of change of angle of attack with elevon deflection at $C_m = 0$, $\partial \alpha / \partial \delta_e$
$(\beta_{\delta_R})_{C_n = 0}$	rate of change of angle of sideslip with rudder deflection at $C_n = 0$, $\partial \beta / \partial \delta_R$

Configuration symbols:

W	wing
B	body
C_1	blunt-canopy, inclined 30°
C_7	vee-canopy
P	nose probe
N_3	blunt, interim nose shape
N_4	pointed, final nose shape
VT_{60}	vertical tail, 60° sweptback leading edge, 5° swept-forward trailing edge
VT_{60-1}	vertical tail, 60° sweptback leading edge, 0° swept-forward trailing edge
D_0	inlets open

D_F	inlets closed with faired plugs
D_F^O	inlets open and closed
F	chordwise wing fences on
F_W^O	chordwise wing fences both on and off

MODEL AND APPARATUS

The tests were conducted in the Langley 4- by 4-foot supersonic pressure tunnel at $M = 1.41$ and 2.01 .

The 1/20-scale model of the Convair MX-1554 airplane used in this investigation is shown in figure 2. Details of the model (which was supplied by the contractor) are given in table I. The basic configuration for the present (designated herein as Phase II) tests had a 60° delta wing mounted on the short fuselage in a mid-low position and had NACA 0004-65 (mod.) airfoil sections. The vertical tail was similar in plan form and section to the wing semispan. The model was equipped with wing trailing-edge flaps and a rudder. The configuration had chordwise wing fences and a probe projecting from the nose. Twin ram-type inlets were located well forward on the sides of the fuselage, but for the present tests (Phase II) the inlets were closed by means of faired plugs. The blunt interim nose N_3 and the blunt 30° optical flat canopy C_1 tested as part of the Phase I basic configuration were replaced by a pointed nose shape N_4 and a sharp-leading-edge vee-canopy C_7 for the Phase II tests.

Three different afterbodies (fig. 3) were tested: a short symmetrical afterbody (which was part of the basic configuration); an elongated symmetrical afterbody; and an elongated upswept afterbody, designed to provide ground clearance. The latter two afterbodies, which have base areas approximately the same as the base area of the short symmetrical afterbody, were designed to provide a more gradual decrease in the cross-sectional area distribution of the complete configuration. Figure 4 presents a series of photographs showing the complete configuration with the different afterbodies installed. The cross-sectional area distribution of the complete model with the various afterbodies is given in figure 5.

A body of revolution (fig. 6) having the same cross-sectional area distribution as the complete basic configuration ($WBPFN_4C_7VT_{60}D_F$ + Short symmetrical afterbody) was tested to provide additional data for area-rule consideration.

Forces and moments were measured by means of a six-component internal strain-gage balance and indicating system.

TESTS

The model was mounted on a 4° bent sting which enabled pitch tests to be made through an angle-of-attack range from -4° to 12° at $\beta = 0^\circ$ and sideslip tests to be conducted through a range of sideslip angles from -4° to 12° at 0° and 4° angle of attack.

The various conditions for the tests were:

Mach number	Reynolds number, based on M.A.C.	Stagnation pressure, lb/sq in. abs.	Stagnation temperature, $^\circ\text{F}$
1.41	1.37×10^6	4	100
	3.08	9	100
	4.80	14	100
	7.02	21	110
	8.83	27	120
2.01	1.13	4*	100
	2.55	9	100
	3.96	14	100
	5.83	21	108
	7.27	27	120

*For this low stagnation pressure, the test section Mach number was approximately 1.97.

The stagnation dew point for the test was less than -25°F .

CORRECTIONS AND ACCURACY

The angles of attack and sideslip have been corrected for deflections of the balance and sting caused by the aerodynamic loads and are estimated to be accurate within $\pm 0.2^\circ$. The estimated accuracy of the control-deflection settings was $\pm 0.1^\circ$.

No corrections were made for Mach number gradient and flow angularity. It should be noted that center-line calibration measurements of the $M = 2.0$ nozzle indicate that the free-stream Mach number drops to 1.97 at $p_0 = 4$ lb/sq in. abs. Accordingly, the low Reynolds number data

have been computed for a free-stream $M = 1.97$. Inasmuch as this change in M is small, the data are presented on the $M = 2.01$ plots. The variations of Mach number and flow angularity are:

	$M = 1.41$	$M = 2.01$	
	p_o , lb/sq in. abs.	p_o , lb/sq in. abs.	
	4, 9, 14, 21, 27	4	9, 14, 21, 27
Mach number variation in nozzle	± 0.01	1.97 ± 0.015	± 0.01
Air-stream angularity in horizontal plane, deg	+0.0 -0.25	± 0.05	± 0.05
Air-stream angularity in vertical plane, deg	+0.15 -0.25	± 0.1	± 0.05

The estimated errors in the coefficients are as follows:

C_L	± 0.005
C_X	± 0.001
C_m	± 0.002
C_Y	± 0.003
C_n	± 0.0002
C_l	± 0.0002

Base-pressure measurements were made for all tests and the longitudinal-force coefficients were corrected to correspond to a base pressure equal to free-stream static pressure. It is believed that sting interference effects on the upswept afterbody are small and that the changes in the upswept afterbody (fig. 3) to provide sting clearance had little effect on the aerodynamic characteristics.

PRESENTATION OF RESULTS

The results of the investigation are presented in figures 7 to 16 as follows:

Data presentedLongitudinal characteristicsFigure

Pitch tests, with various elevon deflections, of the complete configuration with the short symmetrical afterbody, the elongated symmetrical afterbody, and the elongated unswept afterbody.

7

- (a) $M = 1.41$; $R = 4.80 \times 10^6$
(b) $M = 2.01$; $R = 3.96 \times 10^6$

Pitch tests of the complete basic configuration (short symmetrical afterbody) at various Reynolds numbers.

8

- (a) $M = 1.41$
(b) $M = 2.01$

Curves of ΔC_D versus C_L^2 for the various test configurations at $M = 1.41$ and 2.01 , $\delta_e = 0^\circ$. Variable R data are presented for the basic configuration.

9

Pitch tests of the complete basic configuration (short symmetrical afterbody), the wing-body combination, and the "equivalent-area" distribution body of revolution. $M = 1.41$; $R = 4.8 \times 10^6$.

10

Lateral characteristics

Sideslip tests at $\alpha = 0^\circ$ of the complete basic configuration (short symmetrical afterbody) with and without the vertical tail.

11

- (a) $M = 1.41$; $R = 4.80 \times 10^6$
(b) $M = 2.01$; $R = 3.96 \times 10^6$

Sideslip tests at $\alpha = 4^\circ$, $\delta_R = 0^\circ$, of the complete configuration with the short symmetrical afterbody, the elongated symmetrical afterbody, and the elongated upswept afterbody.

12

Sideslip test at $\alpha = 4^\circ$, $\delta_R = -15^\circ$, of the complete configuration with the short symmetrical afterbody.

- (a) $M = 1.41$; $R = 4.80 \times 10^6$
(b) $M = 2.01$; $R = 3.96 \times 10^6$

Sideslip tests at $\alpha = 4^\circ$ of the complete basic configuration (short symmetrical afterbody) over a Reynolds number range of 1.13×10^6 to 7.27×10^6 .
 $\delta_R = 0^\circ$; $M = 2.01$. 13

Variation with Mach number

Longitudinal parameters through the supersonic Mach number range. $\beta = 0^\circ$. 14

Longitudinal control parameters through the supersonic Mach number range. $\beta = 0^\circ$. 15

Lateral parameters through the supersonic Mach number range. 16

(a) $\alpha = 0^\circ$

(b) $\alpha = 4^\circ$

The longitudinal parameters $C_{L\alpha}$, C_{mC_L} , C_{Dmin} , $(C_{m\delta_e})_{\alpha=0^\circ}$, $(C_{L\delta_e})_{trim}$, and $(\alpha\delta_e)_{trim}$ are presented in table II and the lateral parameters $C_{Y\beta}$, $C_{l\beta}$, $C_{n\beta}$, and $(\beta\delta_R)_{C_n=0}$ are given in table III. Table IV is a compilation of the values of C_L , C_m , C_X , C_Y , C_l , and C_n measured for the various test configurations and conditions.

DISCUSSION

Longitudinal Characteristics

Basic.— Changing the nose and canopy shapes of the basic configurations from those of reference 1 had little effect on the aerodynamic characteristics; however, some reduction in drag was noted.

Afterbody extensions.— Extending the afterbody length of the complete configuration (fig. 7) caused little change in the minimum longitudinal-force coefficient and in the lift-curve slope at both test Mach numbers. The static margin of the extended afterbody configurations was approximately 0.01 higher than the values of C_{mC_L} for the basic configuration at $M = 1.41$ and 2.01 . The drag due to lift (fig. 9) showed little or no change with afterbody extension at both test Mach numbers.

Reynolds number effects.— The basic configuration was tested over a range of Reynolds numbers at $M = 1.41$ and 2.01 (figs. 8 and 9). Except for a small increase in the drag due to lift at the lowest Reynolds numbers, the Reynolds number effects were negligible. Values of $1/C_{L\alpha}$ (at the higher Reynolds numbers) are higher than $\Delta C_D/C_L^2$ at $M = 1.41$ and about the same as $\Delta C_D/C_L^2$ at $M = 2.01$. (See ref. 4 for further discussion of these data.)

Controls.— Extending the afterbody length improved the elevon effectiveness at $M = 1.41$ but had no effect on $C_{m\delta_e}$ at $M = 2.01$ (table II). The variation of the trim lift coefficient with elevon deflection for the basic configuration was -0.011 and -0.007 at $M = 1.41$ and 2.01 , respectively. The corresponding values of $(\alpha_{\delta_e})_{trim}$ were -0.34 and -0.29 . Deflection of the elevons -10° increased $C_{x_{min}}$ from -0.022 to -0.028 at $M = 1.41$ and from -0.020 to -0.023 at $M = 2.01$; the trim drag coefficient for $\delta_e = -10^\circ$ (fig. 7) was 0.032 at $M = 1.41$ and 0.024 at $M = 2.01$.

Lateral Characteristics

Basic.— The lateral characteristics of the basic configuration were only slightly affected by changing the angle of attack from 0° to 4° (figs. 11 and 12) except at $M = 1.41$, where $C_{l\beta}$ increased from -0.0006 to -0.0012 . At 4° angle of attack, $M = 2.01$, the changes in the lateral parameters were negligible as the Reynolds number was increased above the nominal test value of 3.96×10^6 (fig. 13). A small decrease in $C_{Y\beta}$ and $C_{n\beta}$ was indicated at $R = 1.13 \times 10^6$.

Afterbody extensions.— The effects of the different afterbodies on the lateral characteristics of the complete model at $\alpha = 4^\circ$ are presented in figure 12 for $M = 1.41$ and 2.01 . Increasing the afterbody length improved the directional stability and increased $C_{Y\beta}$ for the complete configuration at both test Mach numbers without affecting $C_{l\beta}$ in the range $-4^\circ < \beta < +4^\circ$. The parameters $C_{n\beta}$, $C_{Y\beta}$, and $C_{l\beta}$ decreased with increasing Mach number for all configurations (table III).

Controls.— Rudder deflections at $\alpha = 4^\circ$ ($M = 1.41$ and 2.01) caused little change in $C_{Y\beta}$, $C_{l\beta}$, and $C_{n\beta}$ (fig. 12). A value

of $(\beta_{\delta_R})_{C_n = 0} = -0.3$ was measured at $M = 1.41$. At $M = 2.01$, however, no value of $(\beta_{\delta_R})_{C_n = 0}$ could be measured with $\delta_R = -15^\circ$ because of the low value of $C_{n\beta}$.

Variation of Aerodynamic Parameters With Mach Number

Figures 14 to 16 are presented to show the correlation and variation of the longitudinal and lateral parameters with Mach number for the Convair MX-1554 configuration.

In general, the correlation of the data between the various test facilities is good except for some scatter in the drag results. There is some question, however, whether certain of these drag data are corrected for internal flow and base drag (fig. 14). The 4- by 4-foot supersonic pressure tunnel value of $C_{D_{min}}$ at $M = 2.01$ was lower for the second phase tests than for the Phase I (ref. 1) tests. This reduction is believed due to the changes in the basic canopy and nose shapes.

The values of the "tail-on" effective dihedral parameter from reference 3 are lower than the $C_{l\beta}$ values from the other facilities at $M = 1.22$ and 1.56 (fig. 16(a), $\alpha = 0^\circ$).

Figure 16(b) presents the values of the lateral parameters at $\alpha = 4^\circ$ obtained from tests of the Convair MX-1554 in the 4- by 4-foot supersonic pressure tunnel at $M = 1.41, 1.61$, and 2.01 . The change in the directional stability (between the Phase I and Phase II tests) indicated by the individual fairing of the $C_{n\beta}$ curves versus M is within the experimental accuracy but may be due in part to changes in the nose shape, canopy shape, and inlet openings of the basic configuration between the Phase I and Phase II tests. In any case, $C_{n\beta}$ is approaching 0 near $M = 2.0$ (fig. 16(b)).

CONCLUDING REMARKS

The results of the present tests of the Convair MX-1554 at $M = 1.41$ and 2.01 indicate that extension of the fuselage afterbody length caused little change in the minimum longitudinal-force coefficient and in the drag due to lift. Elongating the afterbody resulted in slight increases in the static longitudinal stability, static lateral stability, and side force and had negligible effect on the other parameters.

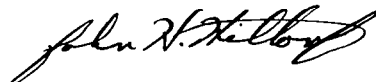
~~CONFIDENTIAL~~

The variation of trim lift coefficient with elevon deflection for the basic configuration decreased from -0.011 at $M = 1.41$ to -0.007 at $M = 2.01$.

The data indicated a value of -0.3 for $(\beta_{\delta R})_{C_n = 0}$ at $M = 1.41$, $\alpha = 4^\circ$. The directional stability of the basic configuration decreases with increasing Mach number and is approaching zero near $M = 2.0$, $\alpha = 4^\circ$.

Reynolds number effects were small; however, some increase in $\Delta C_D / C_L^2$ was indicated at low Reynolds numbers for both test Mach numbers.

Langley Aeronautical Laboratory,
National Advisory Committee for Aeronautics,
Langley Field, Va., July 28, 1953.



John H. Hilton, Jr.
Aeronautical Research Scientist



Edward B. Palazzo
Aeronautical Engineer

Approved:



John V. Becker
Chief of Compressibility Research Division

DRY

REFERENCES

1. Hilton, John H., Jr., Hamilton, Clyde V., and Lankford, John L.: Preliminary Wind-Tunnel Investigation of a 1/20-Scale Model of the Convair MX-1554 at Mach Numbers of 1.61 and 2.01. NACA RM SL52L11a, U. S. Air Force, 1952.
2. O'Brien, Norman R.: Summary of Wind Tunnel Test Results for the F-102 Airplane at Mach 1.20 in the Coop Wind Tunnel Utilizing a 1/20th Scale Model. Aero Memo A-8-8 (Revision A), Consolidated Vultee Aircraft Corp., Feb. 20, 1952.
3. Anon.: Supersonic Wind Tunnel Tests of an .016 Scale Model of the F-102 Airplane in the NOL 40cm x 40cm Wind Tunnel. Part I: Evaluation of the Preliminary Configuration. Aero Memo A-8-17, Consolidated Vultee Aircraft Corp., May 16, 1952.
4. Osborne, Robert S., and Kelly, Thomas C.: A Note on the Drag Due to Lift of Delta Wings at Mach Numbers up to 2.0. NACA RM L53A16a, 1953.

TABLE I.- DIMENSIONAL DATA FOR A 1/20-SCALE MODEL OF
THE CONVAIR MX-1554 AIRPLANE

Wing:

Area, sq ft	1.625
Span, in.	22.68
Mean aerodynamic chord, in.	13.755
Aspect ratio	2.20
Taper ratio	0
Root chord, in.	20.64
Tip chord, in.	0
Airfoil section	NACA 0004-65 (mod.)
Angle of incidence, deg	0
Dihedral angle, deg	0
Sweepback of leading edge, deg	60
Sweepforward of trailing edge, deg	5
Leading-edge radius in percent chord (measured streamwise)	0.18

Vertical tail:

Area (exposed), sq in.	24.57
Span, in.	5.2
Aspect ratio (panel)	1.1
Taper ratio	0
Root chord, in.	9.44
Tip chord, in.	0
Airfoil section	NACA 0004-65 (mod.)
Sweepback of leading edge, deg	60
Sweepforward of trailing edge, deg	5

Fuselage:

Length with short symmetrical afterbody, in.	30.7
Length with elongated symmetrical afterbody, in.	33.0
Length with elongated upswept afterbody, in.	33.0
Maximum width, in.	3.7
Maximum height (without canopy), in.	3.7
Base area, short symmetrical afterbody, sq in.	5.10
Base area, elongated symmetrical afterbody, sq in.	5.05
Base area, elongated, upswept afterbody, sq in.	5.97



TABLE II.- LONGITUDINAL PARAMETERS OF THE CONVAIR MX-1554 MODEL AT $M = 1.41$ AND 2.01

				Longitudinal parameters													
Configuration				M = 1.41							M = 2.01						
	δ_e , deg	δ_R , deg	β , deg	Reynolds number	$C_{L\alpha}$	C_{mC_L}	$C_{D_{min}}$	$(C_{L\alpha})_{trim}$	$(\alpha_{0e})_{trim}$	$(C_{m\alpha})_{\alpha=0^\circ}$	Reynolds number	$C_{L\alpha}$	C_{mC_L}	$C_{X_{min}}$	$(C_{L\alpha})_{trim}$	$(\alpha_{0e})_{trim}$	$(C_{m\alpha})_{\alpha=0^\circ}$
W + B + P + F + N _h + C ₇ + VT ₆₀ + D _F + Short symmetrical afterbody	0 0 0 0 -10	0 0 0 0 0	0 0 0 0 0	1.37 × 10 ⁶ 3.08 4.80 7.02 8.83 4.80	0.046 .046 .046 .046 .046 .047	-0.198 -.198 -.198 -.198 -.198 -.202	0.022 .022 .022 .022 .022 .028				1.13 × 10 ⁶ 2.55 3.96 5.83 7.27 3.96	0.033 .033 .033 .033 .033 .034	-0.179 -.179 -.179 -.179 -.179 -.184	-0.020 -.020 -.020 -.020 -.020 -.023			
W + B + P + F + N _h + C ₇ + VT ₆₀ + D _F + Elongated symmetrical afterbody	0 -10	0 0	0 0	4.80 4.80	.047 .047	-.209 -.210	.022 .028	-.012	-.36	-.0034	3.96 3.96	.034 .034	-.192 -.194	-.020 -.023	-.007	-.30	-.0019
W + B + P + F + N _h + C ₇ + VT ₆₀ + D _F + Elongated upswept afterbody	0	0	0	4.80	.047	-.210	.022				3.96	.034	-.192	-.020			
W + B + F + N _h + D _F + Short symmetrical afterbody	0		0	4.80	.046		.019										
"Equivalent-area" body of revolution			0	4.80			.019										




TABLE III.- LATERAL PARAMETERS OF THE CONVAIR MX-1554 MODEL AT $M = 1.41$ AND 2.01

				Lateral parameters									
Configuration				M = 1.41					M = 2.01				
	δ_e , deg	δ_R , deg	α , deg	Reynolds number	C_{Y_β}	C_{l_β}	C_{n_β}	$(\beta_{0R})_{C_R=0}$	Reynolds number	C_{Y_β}	C_{l_β}	C_{n_β}	$(\beta_{0R})_{C_R=0}$
W + B + P + F + N ₄ + C ₇ + VT ₆₀ + D _F + Short symmetrical afterbody	0	0	3.9	4.80 × 10 ⁶	-0.0089	-0.0012	0.0011		1.13 × 10 ⁶	-.0069	-.0004	.0002	
	0	0	3.9										
	0	0	3.9										
	0	0	3.9										
	0	-15	3.9										
	0	0	0	4.80	-.0091	-.0012	.0011	-0.3	3.96	-.0074	-.0004	.0003	
	0	0	0	4.80	-.0093	-.0006	.0011		3.96	-.0081	-.0004	.0003	
W + B + P + F + N ₄ + C ₇ + D _F + Short symmetrical afterbody	0		0	4.80	-.0020	.0002	-.0014		3.96	-.0026	-.0004	-.0013	
W + B + P + F + N ₄ + C ₇ + VT ₆₀ + D _F + Elongated symmetrical afterbody	0	0	3.9	4.80	-.0089	-.0012	.0014		3.96	-.0078	-.0004	.0005	
W + B + P + F + N ₄ + C ₇ + VT ₆₀ + D _F + Elongated upswept afterbody	0	0	3.9	4.80	-.0089	-.0012	.0013		3.96	-.0078	-.0004	.0004	





TABLE IV.- TABULATED COEFFICIENTS FROM TESTS OF A 1/20-SCALE MODEL
OF THE MX-1554 AIRPLANE

16

M	Configuration	R	α , deg	β , deg	C_L	C_X	C_m	C_l	C_n	C_Y
1.41	WBPFN ₄ C ₇ VT ₆₀ D _F + Short symetrical afterbody $\delta_e = 0^\circ$; $\delta_R = -15^\circ$	4.80×10^6	4.0	-4.08	0.182	-0.035	-0.035	0.0033	0.0008	0.027
				-2.05	.182	-.036	-.035	.0008	.0031	.008
				-.03	.182	-.036	-.035	-.0012	.0049	-.006
				1.99	.181	-.036	-.034	-.0042	.0076	-.028
				4.02	.178	-.035	-.034	-.0065	.0099	-.047
				6.05	.174	-.035	-.034	-.0083	.0118	-.066
				8.09	.170	-.035	-.033	-.0096	.0133	-.085
				10.13	.164	-.034	-.033	-.0106	.0143	-.106
				12.18	.156	-.033	-.032	-.0112	.0145	-.126
				6.05	.174	-.035	-.034	-.0082	.0117	-.065
				.98	.181	-.035	-.035	-.0029	.0063	-.018
				-1.04	.182	-.035	-.035	-.0004	.0040	-.000
				-.02	.181	-.036	-.035	-.0016	.0052	-.001
1.41	WBPFN ₄ C ₇ VT ₆₀ D _F + Short symetrical afterbody $\delta_e = \delta_R = 0^\circ$	4.80×10^6	-4.30	0	-.214	-.038	.041	.0002	.0004	.001
				-2.16	-.114	-.027	.021	.0002	.0003	.001
				-.03	-.016	-.023	.002	0	.0004	-.001
				2.11	.082	-.025	-.017	0	.0003	-.001
				4.24	.181	-.034	-.037	-.0001	.0004	-.001
				6.39	.286	-.051	-.057	-.0002	.0004	-.002
				8.51	.378	-.074	-.075	-.0003	.0005	-.003
				10.64	.467	-.104	-.093	-.0002	.0006	-.003
				6.39	.284	-.052	-.057	-.0002	.0004	-.002
				-.04	-.019	-.023	.002	.0001	.0004	0



NACA RM SL53G30

TABLE IV.- TABULATED COEFFICIENTS FROM TESTS OF A 1/20-SCALE MODEL
OF THE MX-1554 AIRPLANE - Continued

M	Configuration	R	α , deg	β , deg	C_L	C_X	C_m	C_l	C_n	C_Y
1.41	WBPFN ₄ C ₇ VT ₆₀ D _F + Short symetrical afterbody $\delta_e = \delta_R = 0^\circ$	7.02×10^6	-4.56 -2.26 -.04 2.16 4.40 6.62 -.05	0	-0.215 -.115 -.014 .083 .192 .292 -.019	-0.038 -.027 -.023 -.025 -.035 -.052 -.023	0.040 .020 .001 -.017 -.039 -.058 .002	0.0001 .0001 -.0001 0 -.0001 -.0002 0	0.0002 .0004 .0003 .0004 .0004 .0004 .0003	0.001 0 -.001 -.001 -.002 -.002 -.001
1.41	WBPFN ₄ C ₇ VT ₆₀ D _F + Short symetrical afterbody $\delta_e = \delta_R = 0^\circ$	8.83×10^6	-3.48 -2.33 -.07 2.22 4.53 -.07	0	-.169 -.116 -.017 .086 .198 -.018	-.032 -.027 -.023 -.025 -.036 -.023	.031 .021 0 -.018 -.039 .002	.0001 .0001 0 -.0001 -.0001 0	.0003 0 0 .0003 .0004 .0002	.001 0 0 -.001 -.002 0
1.41	WBPFN ₄ C ₇ VT ₆₀ D _F + Short symetrical afterbody $\delta_e = \delta_R = 0^\circ$	1.37×10^6	-4.09 -2.06 -.01 2.02 4.07 6.10 8.14	0	-.210 -.115 -.021 .072 .169 .262 .355	-.037 -.026 -.022 -.024 -.034 -.048 -.070	.039 .020 .001 0 0 .0001 0	.0002 .0002 .0001 0 0 .0001 0	.0002 .0002 .0002 .0003 .0003 .0005 .0005	.003 .003 .002 0 0 -.001 -.001





TABLE IV.- TABULATED COEFFICIENTS FROM TESTS OF A 1/20-SCALE MODEL

18

OF THE MX-1554 AIRPLANE - Continued

M	Configuration	R	α , deg	β , deg	C_L	C_X	C_m	C_l	C_n	C_Y
1.41	WBPFN ₄ C ₇ VT ₆₀ D _F + Short symetrical afterbody $\delta_e = \delta_R = 0^\circ$	1.37×10^6	10.18 12.21 6.10 -.01	0	0.439 .524 .257 -.021	-0.097 -.129 -.048 -.022	-0.090 -.107 -.054 .001	-0.0001 -.0002 0 .0002	0.0006 .0005 .0003 .0004	-0.002 -.002 -.001 .002
1.41	WBPFN ₄ C ₇ VT ₆₀ D _F + Short symetrical afterbody $\delta_e = \delta_R = 0^\circ$	3.08×10^6	-4.19 -2.10 -.02 2.07 4.15 6.24 8.32 10.41 12.49 6.23 -.02	0	-.211 -.110 -.018 .077 .176 .271 .370 .457 .541 .270 -.019	-.037 -.026 -.022 -.025 -.034 -.050 -.072 -.101 -.135 -.049 -.022	.040 .020 .002 0 0 0 0 -.0001 -.108 0 -.002	.0002 .0002 0 0 0 0 0 -.0001 -.0001 0 .0001	.0004 .0004 .0004 .0004 .0004 .0005 .0005 .0005 .0006 .0005 .0005	.001 .001 0 0 -.001 -.002 -.002 -.002 -.003 -.002 0
1.41	WBPFN ₄ C ₇ VT ₆₀ D _F + Short symetrical afterbody $\delta_e = \delta_R = 0^\circ$	4.80×10^6	-4.22 -2.09 .04 2.17 4.31	0	-.260 -.159 -.061 .038 .140	-.048 -.035 -.029 -.029 -.036	.074 .053 .033 .012 -.008	.0001 .0001 -.0001 -.0001 -.0003	.0002 .0003 .0002 .0002 .0003	.001 .001 0 -.001 -.001



NACA RM SL53G30

CONFIDENTIAL

TABLE IV.- TABULATED COEFFICIENTS FROM TESTS OF A 1/20-SCALE MODEL
OF THE MX-1554 AIRPLANE - Continued

M	Configuration	R	α , deg	β , deg	C_L	C_X	C_m	C_l	C_n	C_Y
1.41	WBPFN ₄ C ₇ VT ₆₀ D _F + Short symmetrical afterbody $\delta_e = -10^\circ$; $\delta_R = 0^\circ$	4.80×10^6	6.45 8.59 10.70 12.82 6.45 .04	0	0.241 .335 .414 .498 .238 -.063	-0.051 -.072 -.097 -.129 -.050 -.029	-0.028 -.046 -.062 -.079 -.027 .033	-0.0003 -.0005 -.0003 -.0003 -.0003 -.0001	0.0003 .0004 .0005 .0005 .0003 .0002	-0.002 -.003 -.003 -.003 -.002 0
1.41	WBPFN ₄ C ₇ VT ₆₀ D _F + Elongated symmetrical afterbody $\delta_e = -10^\circ$; $\delta_R = 0^\circ$	4.80×10^6	-4.20 -2.08 .06 2.20 4.34 6.49 8.63 10.77 4.34 .05	0	-.262 -.163 -.065 .038 .141 .244 .338 .431 .138 -.066	-.047 -.035 -.028 -.029 -.036 -.051 -.072 -.100 -.036 -.028	.079 .057 .037 .015 -.007 -.028 -.047 -.066 -.006 .036	.0001 .0001 -.0001 .0001 -.0002 -.0003 -.0006 -.0004 -.0002 .0000	.0003 .0004 .0003 .0004 .0004 .0004 .0006 .0006 .0004 .0004	0 0 -.001 -.001 -.002 -.002 -.003 -.003 -.002 -.001



TABLE IV.- TABULATED COEFFICIENTS FROM TESTS OF A 1/20-SCALE MODEL

OF THE MX-1554 AIRPLANE - Continued

M	Configuration	R	α , deg	β , deg	C_L	C_X	C_m	C_l	C_n	C_Y
1.41	WBPFN ₄ C ₇ VT ₆₀ D _F + Elongated symmetrical afterbody $\delta_e = \delta_R = 0^\circ$	4.80×10^6	-4.30	0	-0.216	-0.037	0.043	0.0002	0.0005	0
			-2.16		-.116	-.026	.022	.0002	.0006	0
			-.03		-.016	-.022	.001	.0000	.0005	-.001
			2.09		.083	-.025	-.019	.0000	.0006	-.001
			4.24		.185	-.034	-.040	-.0001	.0006	-.002
			6.37		.290	-.051	-.062	-.0001	.0006	-.002
			8.51		.387	-.075	-.082	-.0002	.0007	-.003
			10.62		.477	-.105	-.102	-.0002	.0008	-.003
			6.38		.293	-.052	-.062	-.0001	.0006	-.002
			-.03		-.014	-.022	.002	.0000	.0006	-.001
1.41	WBPFN ₄ C ₇ VT ₆₀ D _F + Elongated symmetrical afterbody $\delta_e = \delta_R = 0^\circ$	4.80×10^6	3.8	-4.04	.185	-.033	-.039	.0041	-.0053	.037
				-2.03	.185	-.033	-.039	.0021	-.0029	.020
				0	.185	-.033	-.039	-.0003	-.0001	.001
				2.02	.184	-.032	-.039	-.0027	.0026	-.017
				4.04	.181	-.032	-.039	-.0050	.0055	-.037
				6.07	.178	-.032	-.038	-.0067	.0079	-.057
				8.10	.174	-.031	-.038	-.0080	.0102	-.078
				10.14	.167	-.031	-.037	-.0089	.0117	-.100
				12.18	.159	-.030	-.037	-.0093	.0125	-.121
				6.07	.178	-.032	-.038	-.0067	.0079	-.057
				0	.185	-.032	-.039	-.0003	-.0002	.002



TABLE IV.- TABULATED COEFFICIENTS FROM TESTS OF A 1/20-SCALE MODEL

OF THE MX-1554 AIRPLANE - Continued

M	Configuration	R	α , deg	β , deg	C_L	C_X	C_m	C_l	C_n	C_Y
1.41	WBPFN ₄ C ₇ VT ₆₀ D _F + Elongated symmetrical afterbody $\delta_e = \delta_R = 0^\circ$	4.80×10^6	-4.27	0	-0.221	-0.038	0.048	0.0005	0.0009	-0.001
			-2.14		-.120	-.027	.027	.0005	.0010	-.001
			-.01		-.018	-.022	.005	.0004	.0010	-.002
			2.12		.080	-.024	-.015	.0003	.0010	-.002
			4.25		.182	-.033	-.037	.0004	.0009	-.003
			6.38		.286	-.050	-.059	.0003	.0010	-.003
			8.51		.380	-.073	-.078	.0001	.0009	-.003
			10.62		.469	-.102	-.097	.0003	.0010	-.004
			6.38		.284	-.050	-.058	.0003	.0010	-.003
			-.01		-.022	-.022	.006	.0004	.0010	-.002
1.41	WBPFN ₄ C ₇ VT ₆₀ D _F + Elongated symmetrical afterbody $\delta_e = \delta_R = 0^\circ$	4.80×10^6	3.8	-4.05	.179	-.032	-.035	.0046	-.0046	.036
				-2.03	.181	-.032	-.035	.0026	-.0024	.019
				0	.181	-.032	-.035	.0000	.0002	.001
				2.02	.179	-.032	-.035	-.0024	.0026	-.018
				4.04	.176	-.032	-.034	-.0047	.0052	-.037
				6.07	.175	-.032	-.034	-.0065	.0077	-.058
				8.11	.168	-.031	-.033	-.0078	.0096	-.078
				10.14	.162	-.031	-.033	-.0087	.0109	-.099
				12.19	.153	-.030	-.032	-.0093	.0117	-.121
				6.07	.173	-.031	-.034	-.0064	.0075	-.057
			0		.181	-.032	-.035	.0001	.0001	.001



TABLE IV.- TABULATED COEFFICIENTS FROM TESTS OF A 1/20-SCALE MODEL
OF THE MX-1554 AIRPLANE - Continued

M	Configuration	R	α , deg	β , deg	C_L	C_X	C_m	C_l	C_n	C_Y
1.41	WBPFN ₄ C ₇ VT ₆₀ D _F + Short symmetrical afterbody $\delta_e = \delta_R = 0^\circ$	4.80×10^6	3.8	-4.05	0.181	-0.033	-0.036	0.0042	-0.0042	0.035
				-2.03	.182	-.033	-.036	.0022	-.0025	.019
				0	.181	-.033	-.036	-.0003	-.0003	.001
				2.02	.179	-.033	-.036	-.0028	.0018	-.016
				4.05	.178	-.033	-.035	-.0052	.0041	-.035
				6.08	.174	-.032	-.035	-.0069	.0059	-.054
				8.12	.171	-.032	-.035	-.0084	.0072	-.073
				10.15	.164	-.031	-.034	-.0093	.0080	-.093
				12.20	.155	-.030	-.034	-.0098	.0081	-.114
				6.08	.174	-.032	-.035	-.0069	.0058	-.054
				0	.181	-.033	-.036	-.0003	-.0004	.002
1.41	WBPFN ₄ C ₇ VT ₆₀ D _F + Short symmetrical afterbody $\delta_e = \delta_R = 0^\circ$	4.80×10^6	-2	-4.05	-.015	-.022	.003	.0022	-.0051	.041
				-2.03	-.017	-.022	.003	.0010	-.0027	.021
				0	-.017	-.023	.003	-.0003	-.0004	.002
				2.02	-.018	-.022	.003	-.0015	.0016	-.016
				4.05	-.019	-.022	.003	-.0027	.0040	-.035
				6.07	-.020	-.022	.003	-.0035	.0063	-.056
				8.10	-.024	-.022	.003	-.0039	.0082	-.076
				10.14	-.028	-.022	.003	-.0040	.0096	-.097
				12.19	-.034	-.021	.003	-.0038	.0103	-.119
				6.07	-.021	-.022	.003	-.0035	.0062	-.055
				-.01	-.018	-.022	.003	-.0002	-.0006	.003



TABLE IV.- TABULATED COEFFICIENTS FROM TESTS OF A 1/20-SCALE MODEL
OF THE MX-1554 AIRPLANE - Continued

M	Configuration	R	α , deg	β , deg	C_L	C_X	C_m	C_z	C_n	C_y
1.41	WBPFN ₄ C ₇ D _F + Short symetrical afterbody $\delta_e = 0^\circ$	4.80×10^6	-0.2	-4.08	-0.011	-0.021	0	-0.0013	0.0055	0.009
				-2.04	-.011	-.021	.001	-.0009	.0026	.005
				0	-.011	-.021	.001	-.0005	0	.001
				2.04	-.011	-.021	0	-.0001	-.0027	-.003
				4.07	-.013	-.021	0	.0004	-.0056	-.008
				6.11	-.014	-.021	0	.0012	-.0083	-.013
				8.16	-.017	-.021	0	.0023	-.0110	-.020
				10.20	-.021	-.021	0	.0036	-.0141	-.029
				12.26	-.025	-.021	0	.0051	-.0174	-.039
				6.11	-.014	-.021	0	.0012	-.0083	-.013
				0	-.014	-.021	.001	-.0005	0	.001
1.41	WBFN ₄ D _F + Short symetrical afterbody $\delta_e = 0^\circ$	4.80×10^6	-4.31	0	-.208	-.034	.037	.0003	-.0001	.001
			-2.18		-.110	-.023	.017	.0002	0	.001
			-.04		-.010	-.019	-.002	.0000	0	0
			2.10		.086	-.022	-.021	.0001	0	0
			3.69		.159	-.028	-.035	.0001	0	0
			6.36		.281	-.048	-.060	.0000	.0001	-.001
			8.50		.381	-.071	-.080	-.0001	.0001	-.002
			10.62		.468	-.100	-.098	.0000	.0001	-.002
			4.24		.187	-.031	-.041	.0001	0	-.001
			-.04		-.012	-.019	-.002	.0001	0	0



TABLE IV.- TABULATED COEFFICIENTS FROM TESTS OF A 1/20-SCALE MODEL

OF THE MX-1554 AIRPLANE - Continued

M	Configuration	R	α , deg	β , deg	C_L	C_X	C_m	C_z	C_n	C_Y
1.41	"Equivalent-area" body of revolution	4.80×10^6	-4.09	-0.1	-0.013	-0.021	-0.009	0	0.0001	0.001
			-2.05		-.010	-.020	-.004	0	.0001	0
			-1.04		-.009	-.020	-.002	0	0	0
			-.01		-.006	-.020	0	0	0	0
			1.00		-.005	-.020	.002	0	0	0
			2.03		-.002	-.019	.005	0	0	0
			4.05		.001	-.020	.009	0	-.0001	-.001
			6.09		.005	-.020	.013	0	-.0001	-.001
			8.13		.011	-.021	.016	0	-.0002	-.001
			10.17		.018	-.023	.020	0	-.0002	-.001
			12.21		.026	-.025	.023	-.0001	-.0004	-.001
			6.09		.005	-.019	.013	0	-.0001	0
			-.01		-.008		0	0	0	0





TABLE IV.- TABULATED COEFFICIENTS FROM TESTS OF A 1/20-SCALE MODEL
OF THE MX-1554 AIRPLANE - Continued

M	Configuration	R	α , deg	β , deg	C_L	C_X	C_m	C_l	C_n	C_Y
2.01	WBPFN ₄ C ₇ VT ₆₀ D _F + Elongated symmetrical afterbody $\delta_e = \delta_R = 0^\circ$	3.96×10^6	-0.03 -4.25 -2.14 2.08 4.18 6.27 8.36 10.46 12.56 6.27 -0.04	0.0	-0.007 -.150 -.079 .065 .134 .199 .263 .324 .385 .197 -.009	-0.020 -.032 -.023 -.022 -.029 -.041 -.057 -.078 -.103 -.041 -.020	-0.005 .022 .008 -.019 -.033 0 0 0 -.0001 -.045 -.005	0.0004 .0004 .0004 .0003 .0001 0 0 0 -.0001 .0001 .0004	0.0001 .0001 .0001 .0001 .0001 0 0 0 .0002 .0002 .0001	0.001 .002 .002 .001 0 0 0 -.001 -.001 0 .001 -.001 .001
2.01	WBPFN ₄ C ₇ VT ₆₀ D _F + Elongated symmetrical afterbody $\delta_e = -10^\circ$; $\delta_R = 0^\circ$	3.96×10^6	-4.23 -2.13 -.02 2.08 4.18 6.28 8.38 10.47 12.57 6.28 -.02	0.0	-.176 -.107 -.034 .042 .109 .176 .239 .301 .366 .175 -.034	-.039 -.029 -.024 -.025 -.030 -.041 -.055 -.074 -.098 -.041 -.024	.041 .028 .014 0 0 -.014 -.027 -.040 -.052 -.064 -.027 .014	.0001 0 .0001 0 0 -.0001 -.0002 -.0003 -.0003 -.0001 -.0001	-.0001 -.0001 -.0001 0 0 .0001 .0001 .0002 .0002 .0001 -.0001	.002 .002 .001 .001 .001 0 0 -.001 -.001 0 .001

CONFIDENTIAL

NACA RM SL53G30





TABLE IV.- TABULATED COEFFICIENTS FROM TESTS OF A 1/20-SCALE MODEL

OF THE MX-1554 AIRPLANE - Continued

M	Configuration	R	α , deg	β , deg	C_L	C_X	C_m	C_l	C_n	C_Y
2.01	WBPFN ₄ C ₇ VT ₆₀ D _F + Elongated symmetrical afterbody $\delta_e = \delta_R = 0^\circ$	3.96×10^6	3.9	-4.05	0.134	-0.029	-0.032	0.0013	-0.0017	0.031
				-2.02	.136	-.029	-.033	.0006	-.0008	.015
				0	.136	-.029	-.032	-.0002	.0001	-.001
				2.03	.135	-.029	-.032	-.0009	.0013	-.017
				4.05	.133	-.029	-.032	-.0016	.0021	-.032
				6.08	.128	-.029	-.031	-.0021	.0027	-.049
				8.11	.123	-.028	-.030	-.0025	.0027	-.067
				10.15	.116	-.028	-.030	-.0028	.0026	-.086
				12.19	.110	-.028	-.029	-.0033	.0022	-.104
				6.08	.127	-.028	-.031	-.0020	.0025	-.049
2.01	WBPFN ₄ C ₇ VT ₆₀ D _F + Short symmetrical afterbody $\delta_e = 0^\circ$; $\delta_R = -15^\circ$	3.96×10^6	3.9	0	.136	-.029	-.032	-.0001	.0002	-.001
				-4.07	.129	-.030	-.029	.0005	.0021	.024
				-2.04	.130	-.030	-.029	-.0002	.0026	.008
				-.01	.131	-.030	-.029	-.0010	.0034	-.007
				2.01	.130	-.030	-.028	-.0019	.0039	-.021
				4.04	.126	-.031	-.028	-.0026	.0046	-.037
				6.07	.125	-.031	-.028	-.0032	.0047	-.052
				8.11	.119	-.031	-.027	-.0036	.0045	-.070
				10.14	.113	-.030	-.027	-.0040	.0038	-.087
				12.19	.106	-.030	-.026	-.0044	.0032	-.105
				6.07	.123	-.030	-.028	-.0032	.0045	-.052
				-.01	.131	-.030	-.029	-.0011	.0032	-.006



CONFIDENTIAL

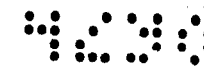


TABLE IV.- TABULATED COEFFICIENTS FROM TESTS OF A 1/20-SCALE MODEL
OF THE MX-1554 AIRPLANE - Continued

M	Configuration	R	α , deg	β , deg	C_L	C_X	C_m	C_l	C_n	C_Y
2.01	WBPFN ₄ C ₇ VT ₆₀ D _F + Short symmetrical afterbody $\delta_e = -10^\circ$; $\delta_R = 0^\circ$	3.96×10^6	-4.23	0	-0.172	-0.038	0.038	0.0002	0	0.001
			-2.13		-.103	-.029	.026	.0002	0	.001
			-.03		-.032	-.024	.013	.0002	.0001	.001
			2.08		.041	-.024	-.001	.0001	0	0
			4.18		.108	-.030	-.013	0	0	0
			6.28		.173	-.040	-.025	-.0001	-.0001	-.001
			8.38		.236	-.054	-.037	-.0001	0	-.001
			10.48		.300	-.073	-.048	-.0002	0	-.001
			12.58		.359	-.097	-.059	-.0002	.0001	-.001
			6.28		.172	-.040	-.025	-.0001	0	-.001
			-.03		-.033	-.024	.013	.0002	0	.001
2.01	WBPFN ₄ C ₇ VT ₆₀ D _F + Short symmetrical afterbody $\delta_e = \delta_R = 0^\circ$	3.96×10^6	-4.24	0	-.145	-.032	.020	.0003	0	.003
			-2.14		-.077	-.024	.008	.0003	0	.002
			-.03		-.006	-.020	-.005	.0003	0	.002
			2.08		.066	-.022	-.017	.0001	0	.002
			4.19		.134	-.029	-.030	0	0	.001
			6.28		.199	-.041	-.042	0	0	.001
			8.38		.262	-.057	-.053	0	.0001	.001
			10.47		.323	-.077	-.065	0	0	0
			12.57		.381	-.101	-.075	-.0001	-.0001	0
			6.28		.197	-.041	-.041	0	0	.001
			-.03		-.006	-.020	-.005	.0003	.0001	.002

NACA



TABLE IV.- TABULATED COEFFICIENTS FROM TESTS OF A 1/20-SCALE MODEL

OF THE MX-1554 AIRPLANE - Continued

M	Configuration	R	α , deg	β , deg	C_L	C_X	C_m	C_l	C_n	C_Y
2.01	WBPFN ₄ C ₇ VT ₆₀ D _F + Short symmetrical afterbody $\delta_e = \delta_R = 0^\circ$	5.83×10^6	-0.05	0	-0.006	-0.020	-0.005	0.0003	0.0001	0.001
			-2.21		-.079	-.023	.008	.0003	.0001	.002
			-4.37		-.147	-.032	.020	.0003	.0001	.002
			2.13		.066	-.022	-.017	.0002	.0002	.001
			4.24		.114	-.028	-.026	.0001	.0002	.001
			6.44		.203	-.042	-.043	.0001	.0002	0
			8.59		.266	-.058	-.054	0	.0001	0
			10.75		.328	-.079	-.065	0	.0001	-.001
			12.89		.387	-.104	-.076	-.0001	.0002	-.001
			6.43		.202	-.039	-.042	0	.0002	0
			-.04		-.007	-.020	-.004	.0003	.0002	.001
2.01	WBPFN ₄ C ₇ VT ₆₀ D _F + Short symmetrical afterbody $\delta_e = \delta_R = 0^\circ$	7.27×10^6	-0.05	0	-.007	-.020	-.004	.0003	.0002	.001
			-4.48		-.148	-.032	.020	.0002	.0001	.002
			-2.28		-.080	-.023	.008	.0002	.0001	.001
			-.05		-.006	-.020	-.004	.0002	.0002	.001
			2.16		.066	-.022	-.017	.0002	.0002	0
			4.36		.136	-.029	-.030	.0001	.0002	0
			6.58		.205	-.042	-.042	.0001	.0002	-.001
			8.77		.270	-.059	-.054	.0001	.0002	-.001
			10.96		.330	-.080	-.065	0	.0002	-.002
			6.57		.204	-.042	-.042	.0001	.0002	-.001
			-.05		-.007	-.020	-.004	.0003	.0002	0

NACA

TABLE IV.- TABULATED COEFFICIENTS FROM TESTS OF A 1/20-SCALE MODEL

OF THE MX-1554 AIRPLANE - Continued

M	Configuration	R	α , deg	β , deg	C_L	C_X	C_m	C_z	C_n	C_Y
2.01	WBPFN ₄ C ₇ VT ₆₀ D _F + Short symmetrical afterbody $\delta_e = \delta_R = 0^\circ$	2.55×10^6	-4.15	0	-0.139	-0.031	0.019	0.0003	0.0001	0.002
			-2.09		-.075	-.023	.008	.0002	.0001	.002
			-.02		-.007	-.019	-.004	.0002	.0002	.001
			2.05		.062	-.021	-.017	.0001	.0001	.001
			4.11		.128	-.028	-.029	.0000	.0001	0
			6.17		.191	-.039	-.040	.0000	.0001	0
			8.24		.251	-.054	-.052	-.0001	.0001	0
			10.30		.309	-.073	-.062	-.0001	.0002	-.001
			12.36		.366	-.096	-.072	-.0003	.0003	-.001
			6.17		.191	-.039	-.040	-.0001	.0001	0
			-.02		-.007	-.019	-.004	.0002	.0002	.001
2.01	WBPFN ₄ C ₇ VT ₆₀ D _F + Short symmetrical afterbody $\delta_e = \delta_R = 0^\circ$	1.13×10^6	-4.08	0	-.139	-.031	.018	.0001	.0001	.002
			-2.04		-.073	-.023	.007	.0003	.0001	.002
			-.01		-.007	-.020	-.004	.0000	.0001	.002
			2.02		.059	-.022	-.016	.0000	-.0001	.002
			4.05		.125	-.028	-.028	-.0001	.0000	0
			6.08		.187	-.039	-.040	-.0001	.0000	0
			8.11		.249	-.054	-.051	-.0003	.0000	0
			10.14		.309	-.073	-.062	-.0003	.0003	0
			12.16		.362	-.095	-.072	-.0003	.0001	0
			6.08		.187	-.039	-.040	-.0003	.0002	0
			-.01		-.007	-.020	-.004	.0000	.0002	0

NACA

TABLE IV.- TABULATED COEFFICIENTS FROM TESTS OF A 1/20-SCALE MODEL

OF THE MX-1554 AIRPLANE - Continued

M	Configuration	R	α , deg	β , deg	C_L	C_X	C_m	C_l	C_n	C_Y
2.01	WBPFN ₄ C ₇ VT ₆₀ D _F + Elongated upswept afterbody $\delta_e = \delta_R = 0^\circ$	3.96×10^6	-4.23	0	-0.153	-0.033	0.026	0.0004	0.0004	0.001
			-2.13		-.082	-.024	.013	.0004	.0004	.001
			-.03		-.010	-.020	-.001	.0004	.0004	0
			2.08		.061	-.022	-.015	.0003	.0004	0
			4.18		.130	-.028	-.028	.0002	.0004	-.001
			6.28		.195	-.040	-.041	.0001	.0004	-.001
			8.37		.259	-.056	-.053	.0001	.0004	-.001
			10.47		.323	-.076	-.066	.0001	.0003	-.001
			12.56		.380	-.100	-.077	.0000	.0002	-.001
			6.28		.195	-.040	-.041	.0001	.0004	-.001
			-.03		-.012	-.020	-.001	.0004	.0004	.001
2.01	WBPFN ₄ C ₇ VT ₆₀ D _F + Elongated upswept afterbody $\delta_e = \delta_R = 0^\circ$	3.96×10^6	3.9	-4.05	.127	-.029	-.028	.0014	-.0013	.030
				-2.02	.129	-.029	-.028	.0008	-.0005	.014
				0	.129	-.028	-.028	.0000	.0004	-.002
				2.03	.128	-.028	-.028	-.0008	.0013	-.017
				4.05	.125	-.028	-.027	-.0015	.0021	-.033
				6.08	.122	-.028	-.027	-.0020	.0026	-.049
				8.11	.117	-.028	-.026	-.0024	.0027	-.067
				10.15	.111	-.028	-.026	-.0027	.0026	-.085
				12.19	.104	-.028	-.025	-.0032	.0022	-.103
				6.08	.122	-.028	-.027	-.0020	.0025	-.049
				0	.129	-.028	-.028	.0000	.0004	-.001



TABLE IV.- TABULATED COEFFICIENTS FROM TESTS OF A 1/20-SCALE MODEL

OF THE MX-155⁴ AIRPLANE - Continued

M	Configuration	R	α , deg	β , deg	C_L	C_X	C_m	C_l	C_n	C_Y
2.01	WBPFN ₄ C ₇ VT ₆₀ D _F + Short symetrical afterbody $\delta_e = \delta_R = 0^\circ$	7.27×10^6	4.0	-4.11 -2.05 .01 2.05 4.11 6.16 8.23 10.32 12.40 6.16 .01	0.134 .136 .136 .134 .132 .128 .123 .117 .109 .128 .136	-0.029 -0.029 -0.029 -0.028 -0.028 -0.028 -0.028 -0.028 -0.027 -0.028 -0.029	-0.030 -0.030 -0.030 -0.030 -0.029 -0.029 -0.029 -0.028 -0.028 -0.029 -0.030	0.0014 .0007 -0.0002 -0.0010 -0.0016 -0.0022 -0.0026 -0.0030 -0.0034 -0.0022 -0.0001	-0.0007 -0.0002 .0003 .0010 .0013 .0015 .0012 .0005 -0.0005 .0014 .0003	0.028 .013 -0.002 -0.017 -0.032 -0.048 -0.064 -0.082 -0.101 -0.047 -0.002
2.01	WBPFN ₄ C ₇ VT ₆₀ D _F + Short symetrical afterbody $\delta_e = \delta_R = 0^\circ$	3.96×10^6	3.9	-4.05 -2.02 0 2.03 4.06 6.08 8.12 10.16 12.20 6.08 0	.129 .130 .130 .129 .127 .124 .118 .114 .106 .124 .130	-0.028 -0.028 -0.028 -0.028 -0.028 -0.028 -0.028 -0.028 -0.027 -0.028 -0.028	-0.029 -0.029 -0.029 -0.029 -0.029 -0.028 -0.028 -0.028 -0.027 -0.028 -0.029	.0014 .0007 -0.0001 -0.0009 -0.0017 -0.0022 -0.0026 -0.0030 -0.0035 -0.0022 -0.0001	-0.0007 -0.0002 .0002 .0009 .0013 .0015 .0012 .0006 -0.0003 .0015 .0002	.027 .012 -0.003 -0.017 -0.033 -0.048 -0.064 -0.082 -0.101 -0.048 -0.002

NACA

TABLE IV.- TABULATED COEFFICIENTS FROM TESTS OF A 1/20-SCALE MODEL

OF THE MX-1554 AIRPLANE - Continued

M	Configuration	R	α , deg	β , deg	C_L	C_X	C_m	C_l	C_n	C_Y
2.01	WBPFN ₄ C ₇ VT ₆₀ D _F + Short symmetrical afterbody $\delta_e = \delta_R = 0^\circ$	1.13×10^6	3.8	-4.01	0.121	-0.028	-0.028	0.0010	-0.0006	0.028
				-2.01	.121	-.028	-.028	.0004	-.0004	.014
				0	.125	-.028	-.029	-.0003	.0000	0
				2.01	.129	-.028	-.029	-.0010	.0005	-.014
				4.01	.125	-.028	-.028	-.0018	.0008	-.028
				6.02	.121	-.028	-.028	-.0021	.0010	-.047
				8.04	.121	-.028	-.028	-.0029	.0011	-.063
				10.05	.118	-.028	-.028	-.0032	.0008	-.081
				12.06	.110	-.028	-.028	-.0035	-.0001	-.099
				6.02	.118	-.028	-.028	-.0021	.0010	-.047
2.01	WBPFN ₄ C ₇ VT ₆₀ D _F + Short symmetrical afterbody $\delta_e = \delta_R = 0^\circ$	3.96×10^6		0	.125	-.028	-.029	-.0003	.0000	0
			-0.2	-4.05	-.013	-.021	-.004	.0013	-.0017	.034
				-2.03	-.012	-.020	-.004	.0008	-.0008	.017
				0	-.012	-.020	-.004	.0000	.0001	.001
				2.02	-.013	-.020	-.003	-.0007	.0011	-.015
				4.05	-.014	-.020	-.003	-.0013	.0020	-.032
				6.07	-.016	-.020	-.003	-.0017	.0025	-.048
				8.11	-.020	-.021	-.003	-.0019	.0026	-.066
				10.15	-.023	-.021	-.003	-.0020	.0025	-.084
				12.19	-.027	-.022	-.004	-.0019	.0019	-.103
				6.07	-.017	-.021	-.003	-.0017	.0024	-.048
				0	-.013	-.021	-.003	.0000	.0001	.001

NACA

TABLE IV.- TABULATED COEFFICIENTS FROM TESTS OF A 1/20-SCALE MODEL
OF THE MX-1554 AIRPLANE - Concluded

M	Configuration	R	α , deg	β , deg	C_L	C_X	C_m	C_l	C_n	C_Y
2.01	WBFFN ₄ C ₇ D _F + Short symmetrical afterbody $\delta_e = 0^\circ$	3.96×10^6	-.2	-4.07	-0.010	-0.020	-0.005	-0.0018	0.0056	0.012
				-2.04	-.009	-.020	-.005	-.0008	.0029	.006
				0	-.009	-.020	-.005	.0000	.0002	.001
				2.03	-.009	-.019	-.005	.0008	-.0026	-.004
				4.07	-.010	-.020	-.005	.0017	-.0053	-.010
				6.10	-.012	-.021	-.005	.0028	-.0081	-.017
				8.14	-.014	-.021	-.005	.0038	-.0109	-.026
				10.19	-.017	-.022	-.006	.0050	-.0138	-.037
				12.24	-.022	-.023	-.006	.0060	-.0167	-.050
				6.10	-.012	-.021	-.005	.0027	-.0081	-.018
				0	-.010	-.019	-.004	.0000	.0002	.001

NACA

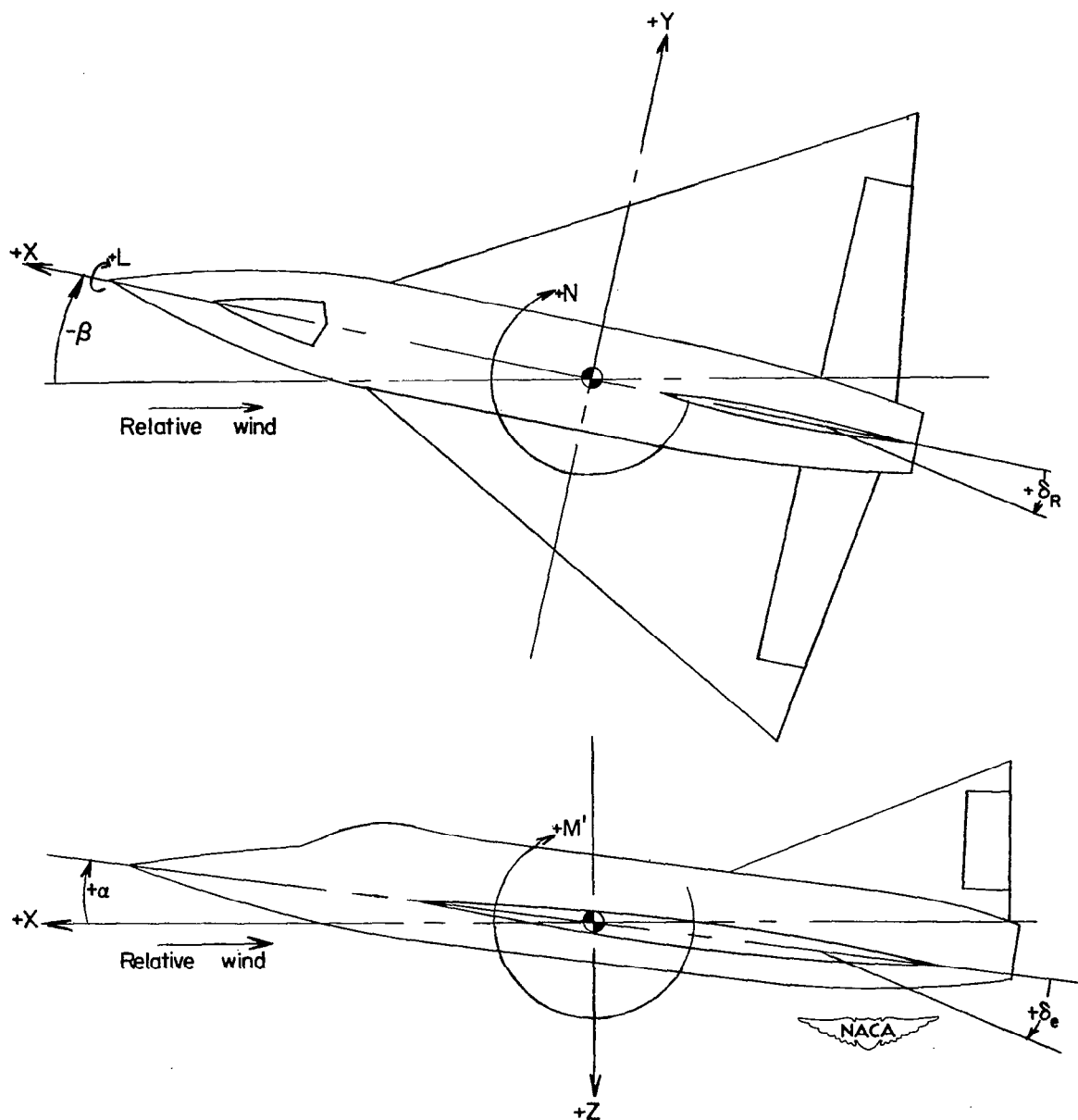


Figure 1.- System of stability axes.

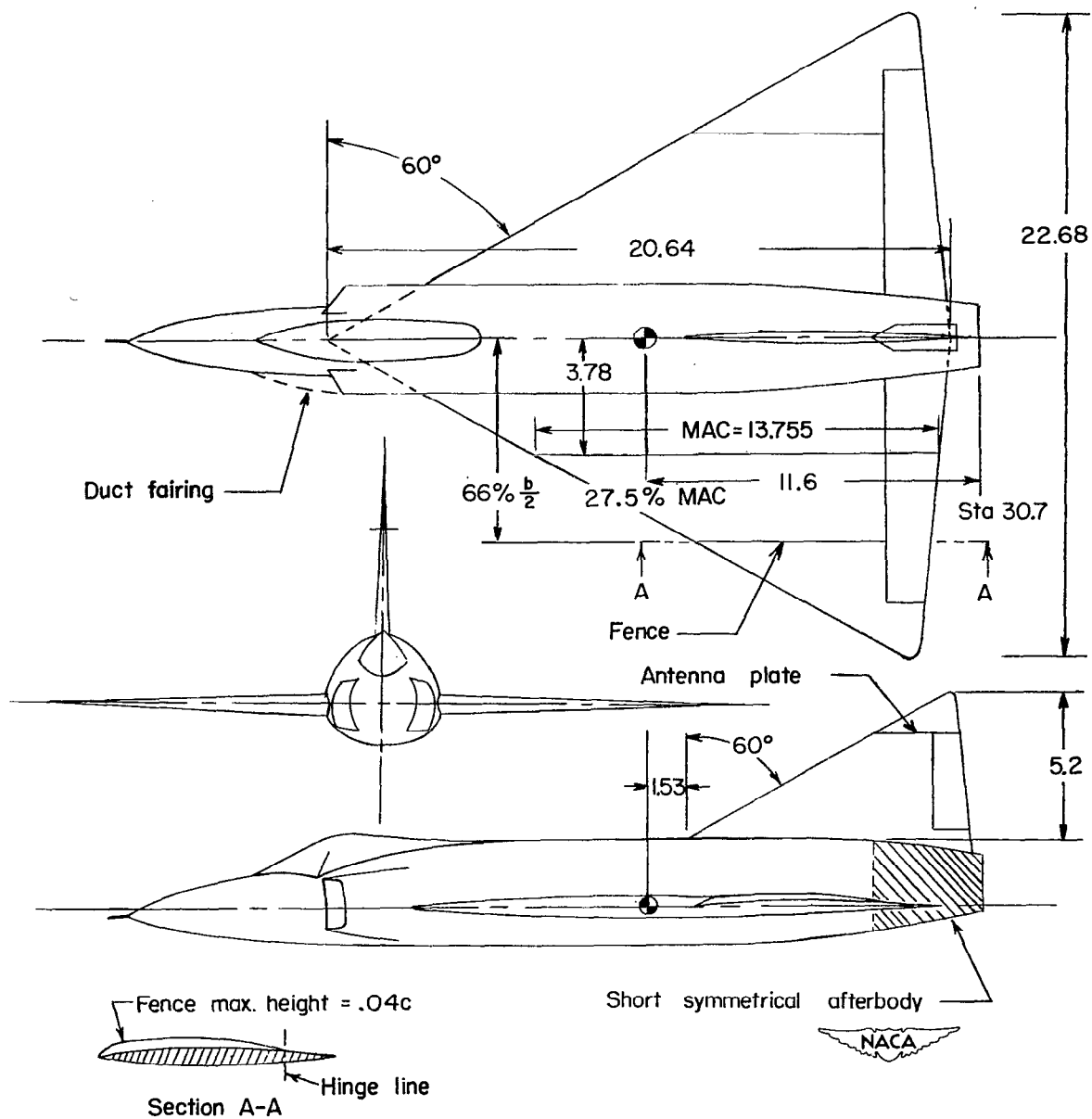


Figure 2.- Three-view sketch of 1/20-scale MX-1554 model. (Dimensions in inches unless noted.)

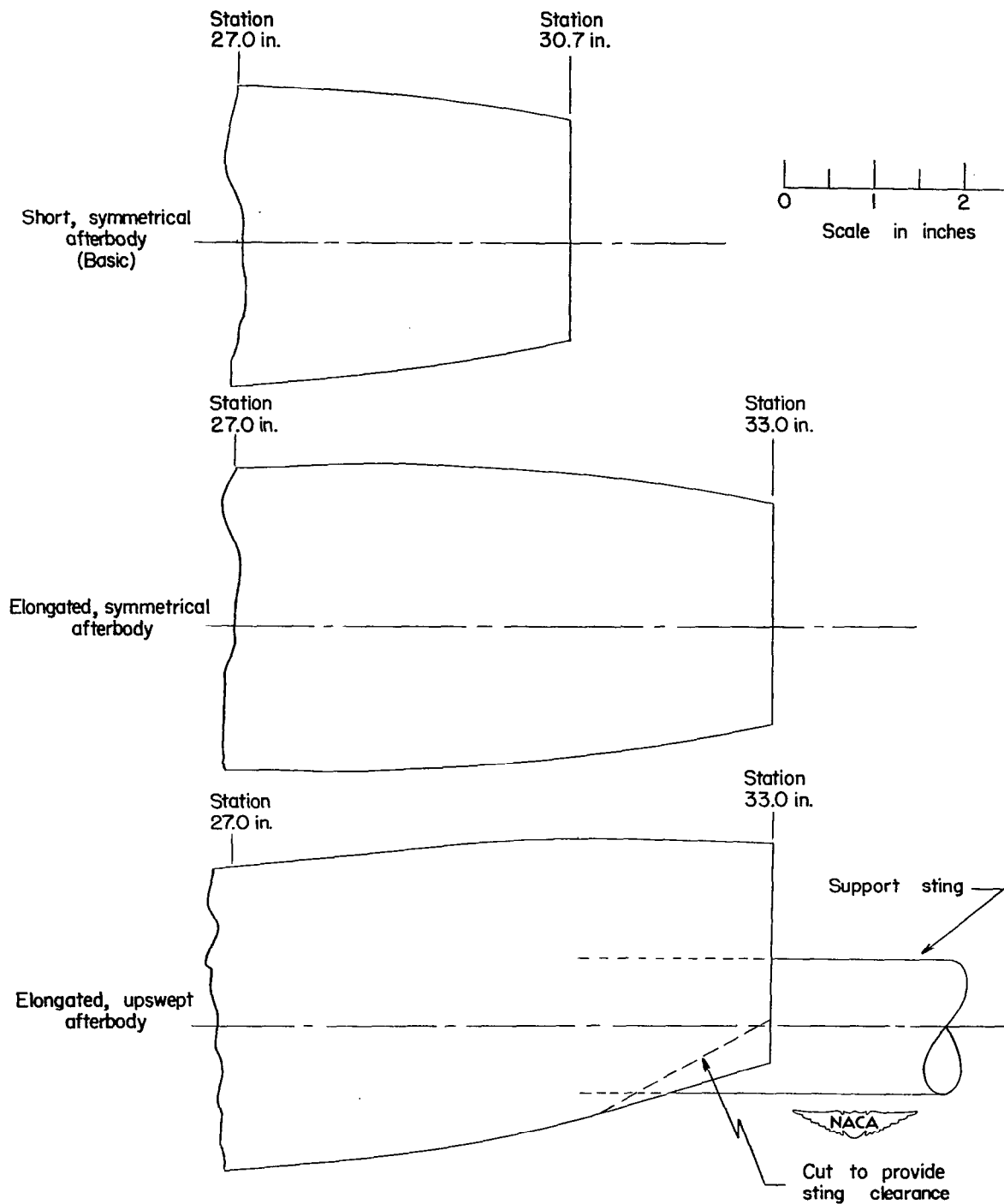
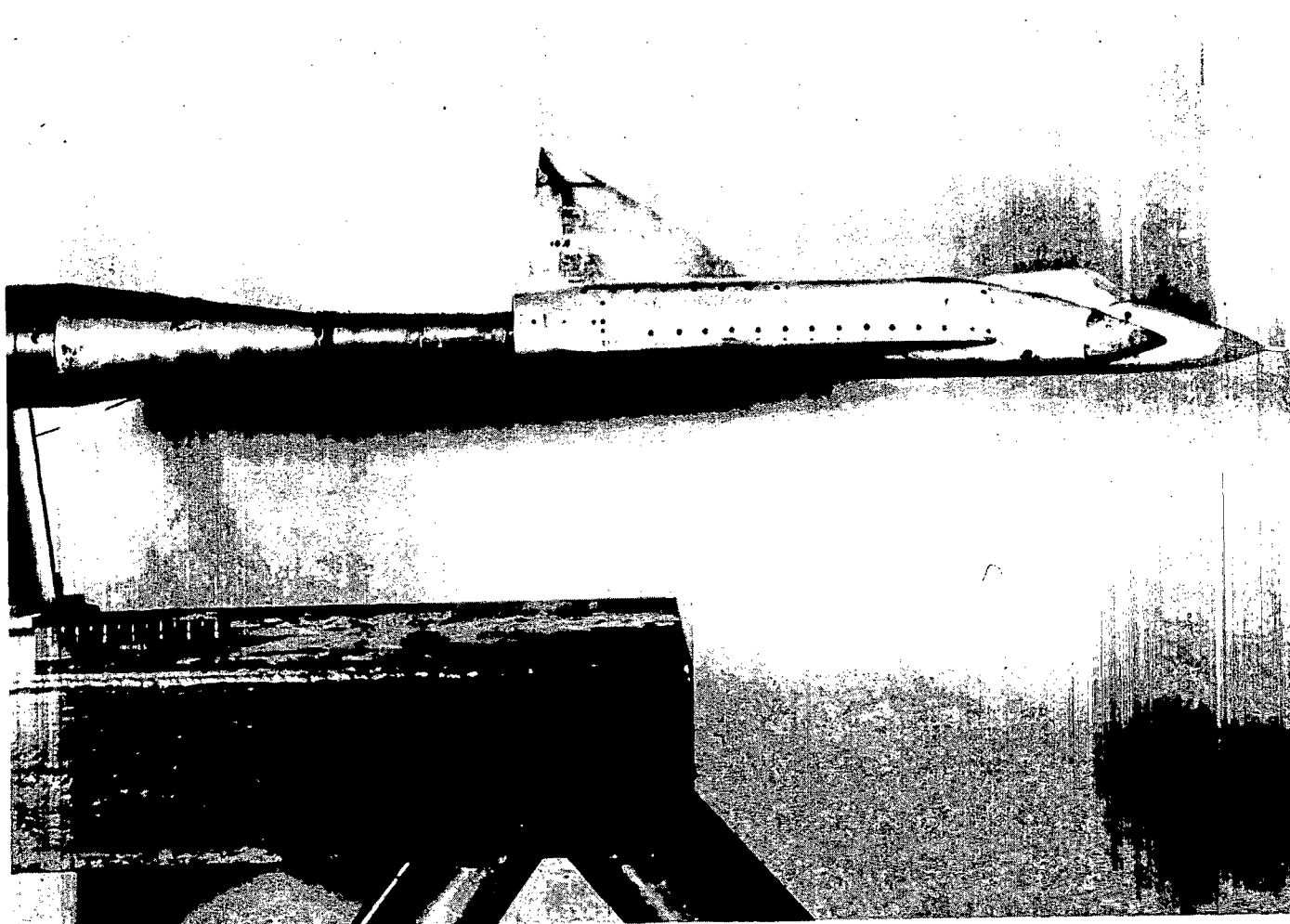


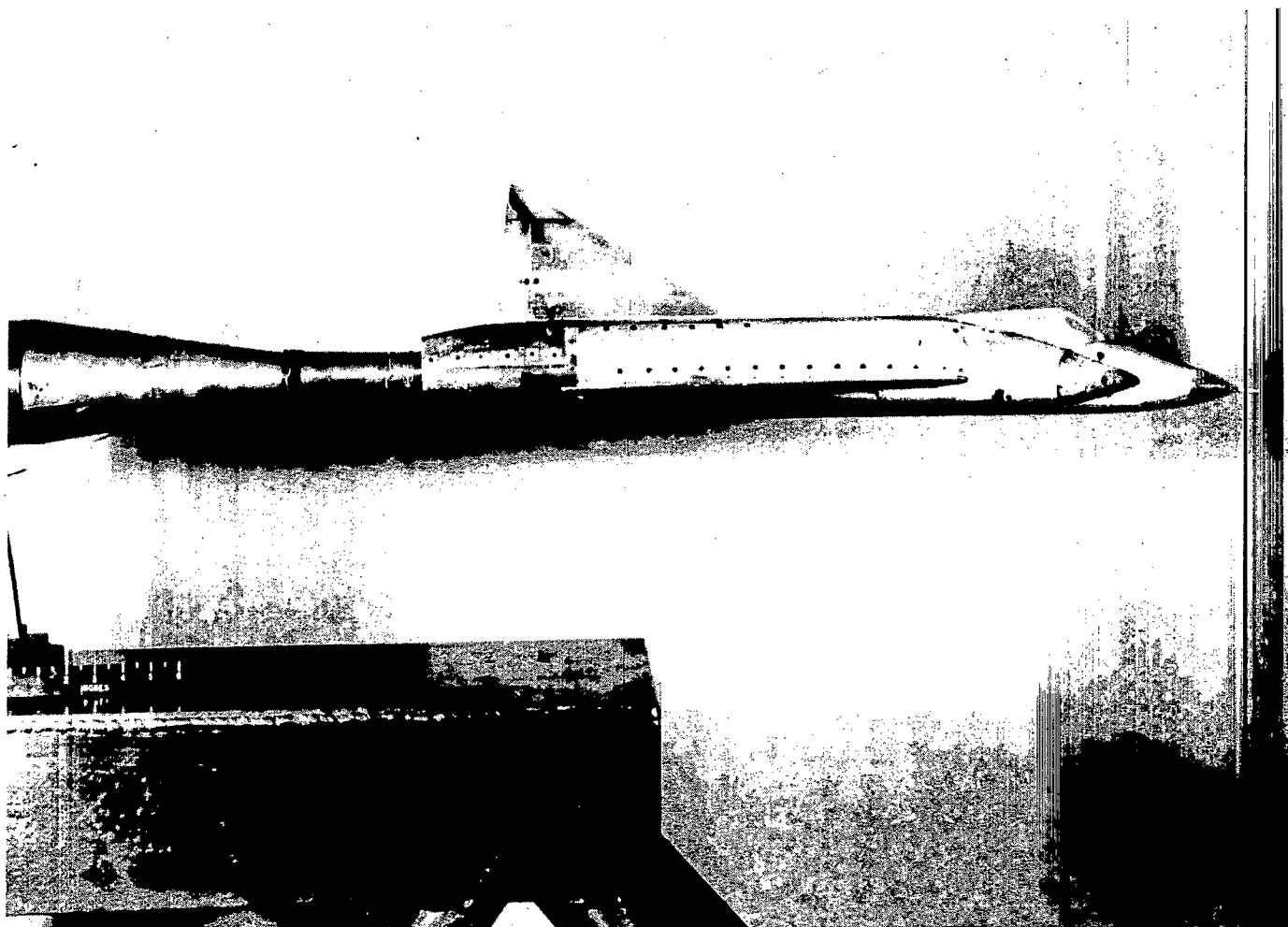
Figure 3.- Side-view sketch of 1/20-scale MX-1554 model afterbodies.



L-78008

(a) Short symmetrical afterbody.

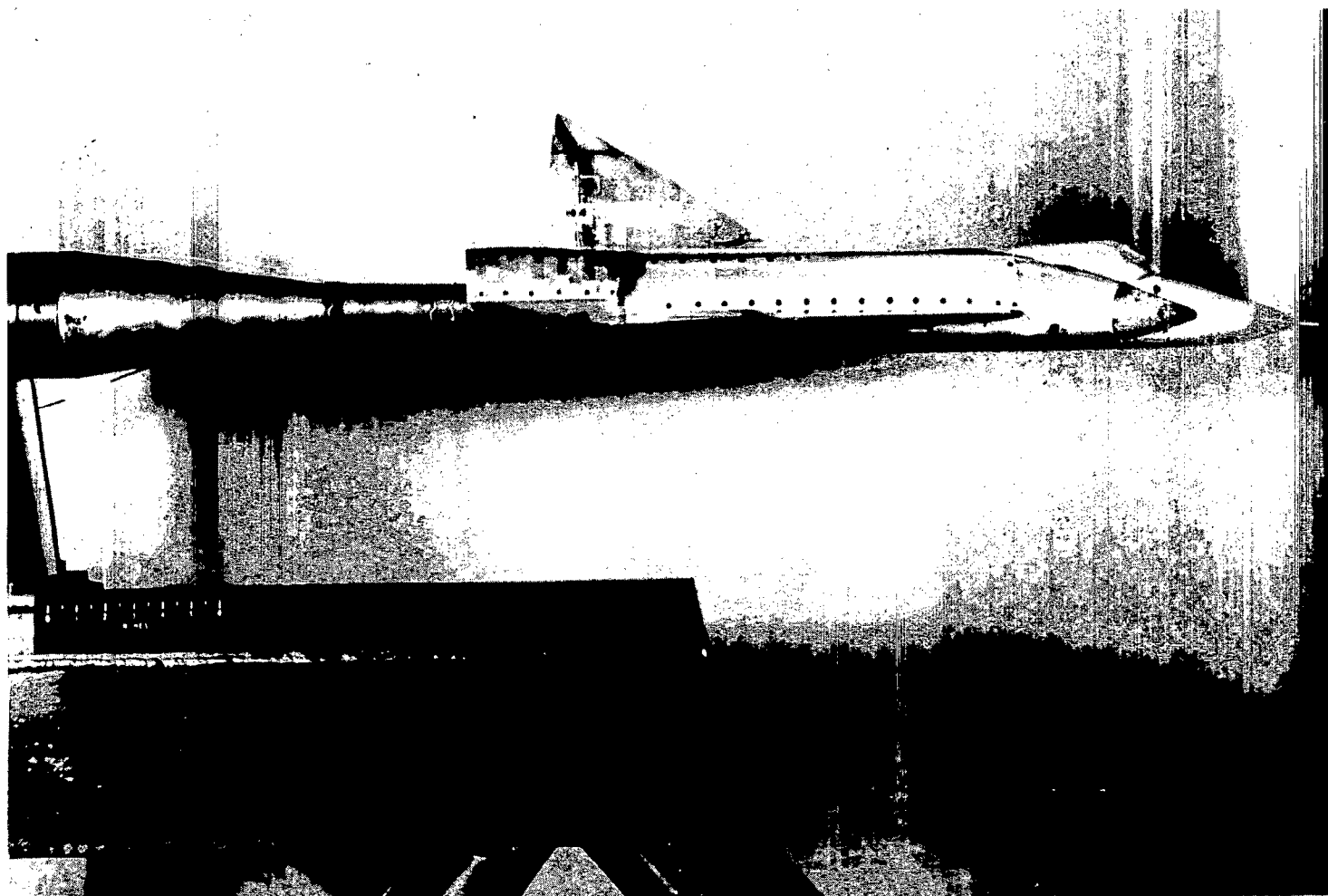
Figure 4.- Photographs of complete MX-1554 model with different afterbodies.



L-78007

(b) Elongated symmetrical afterbody.

Figure 4.- Continued.

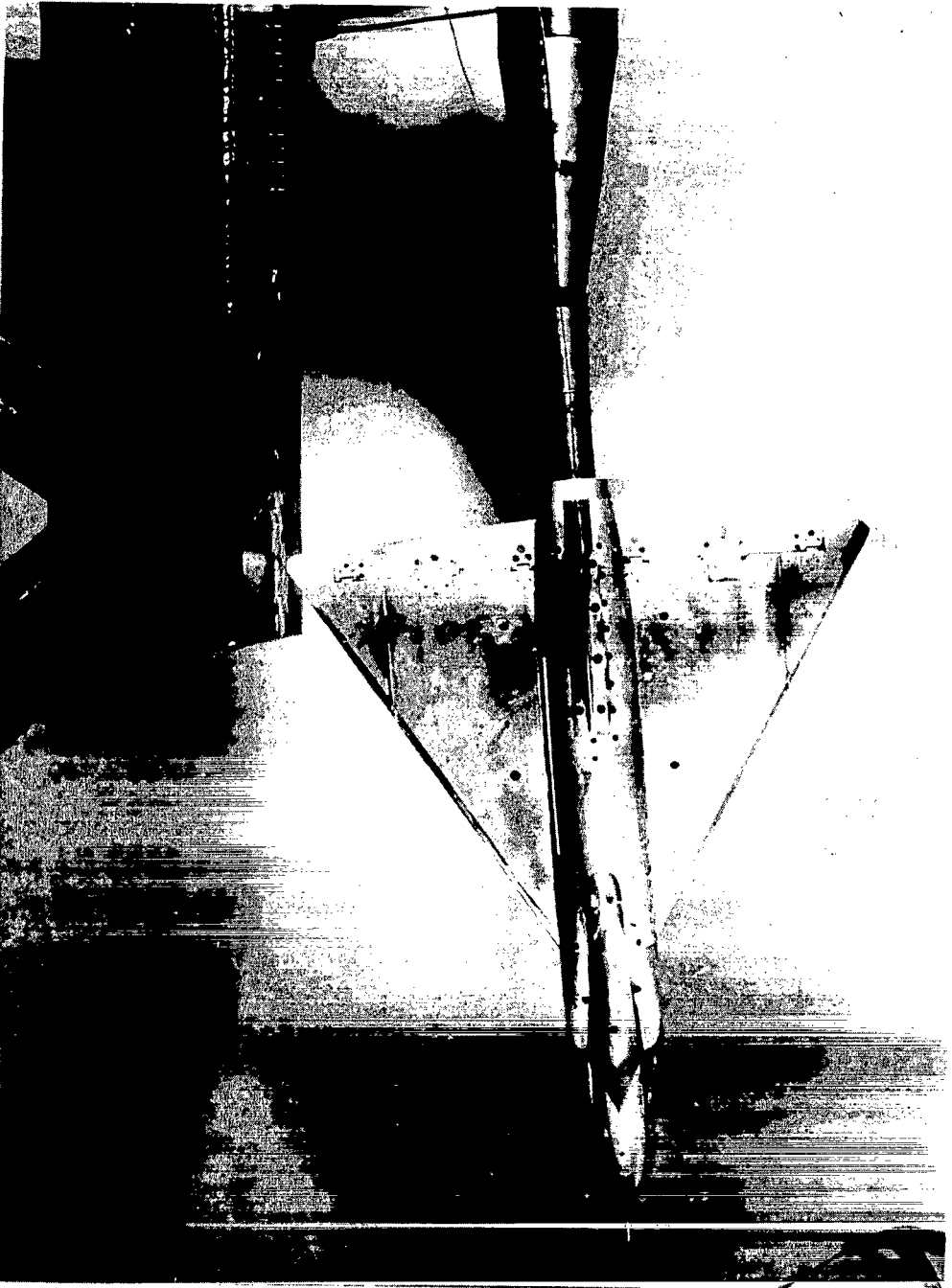


L-78009

(c) Elongated upswept afterbody.

Figure 4.- Continued.

CONFIDENTIAL



(d) Plan view of short symmetrical afterbody.

Figure 4.- Concluded.

L-78011

CONFIDENTIAL

4290 5

CONFIDENTIAL

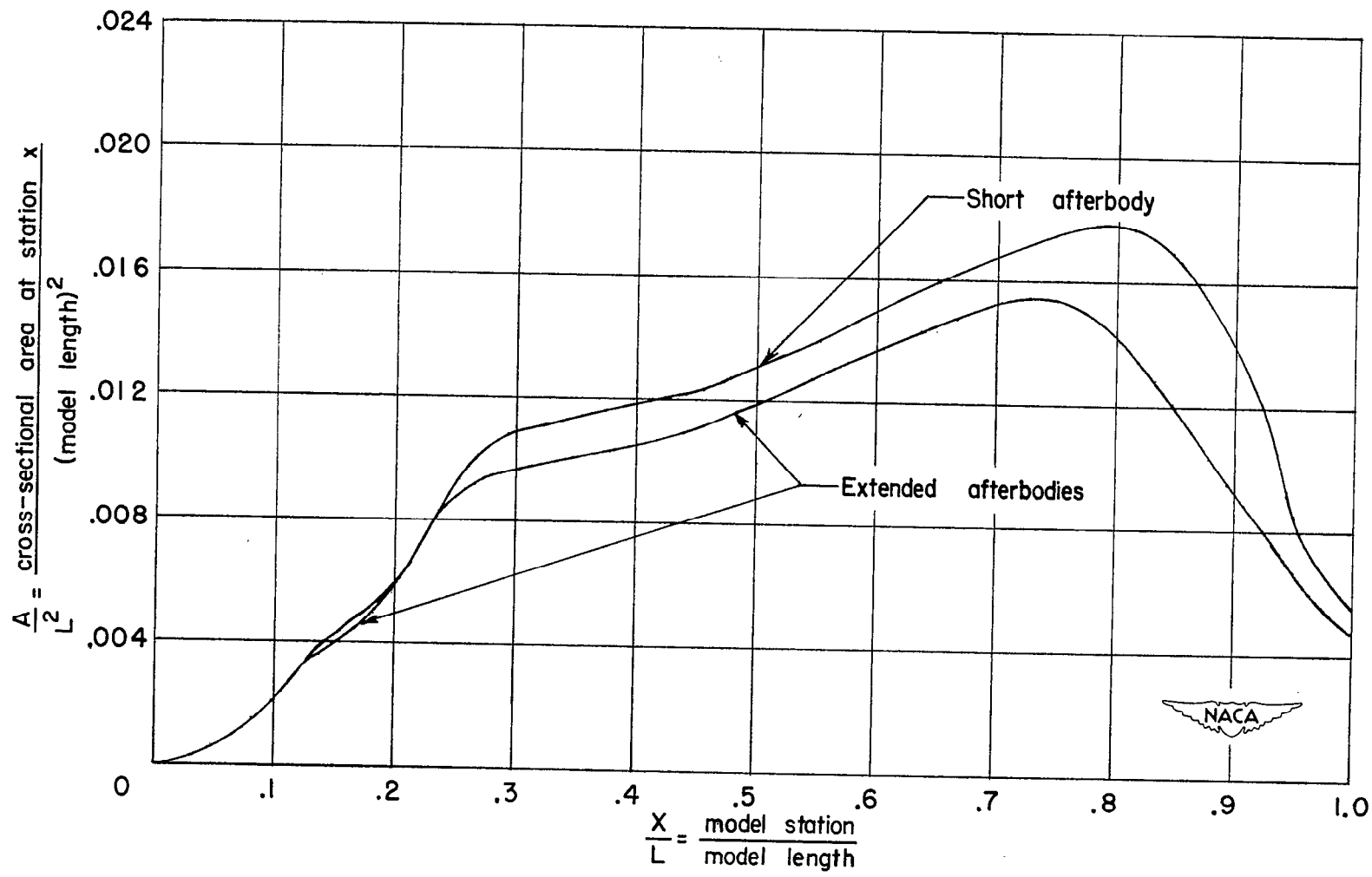
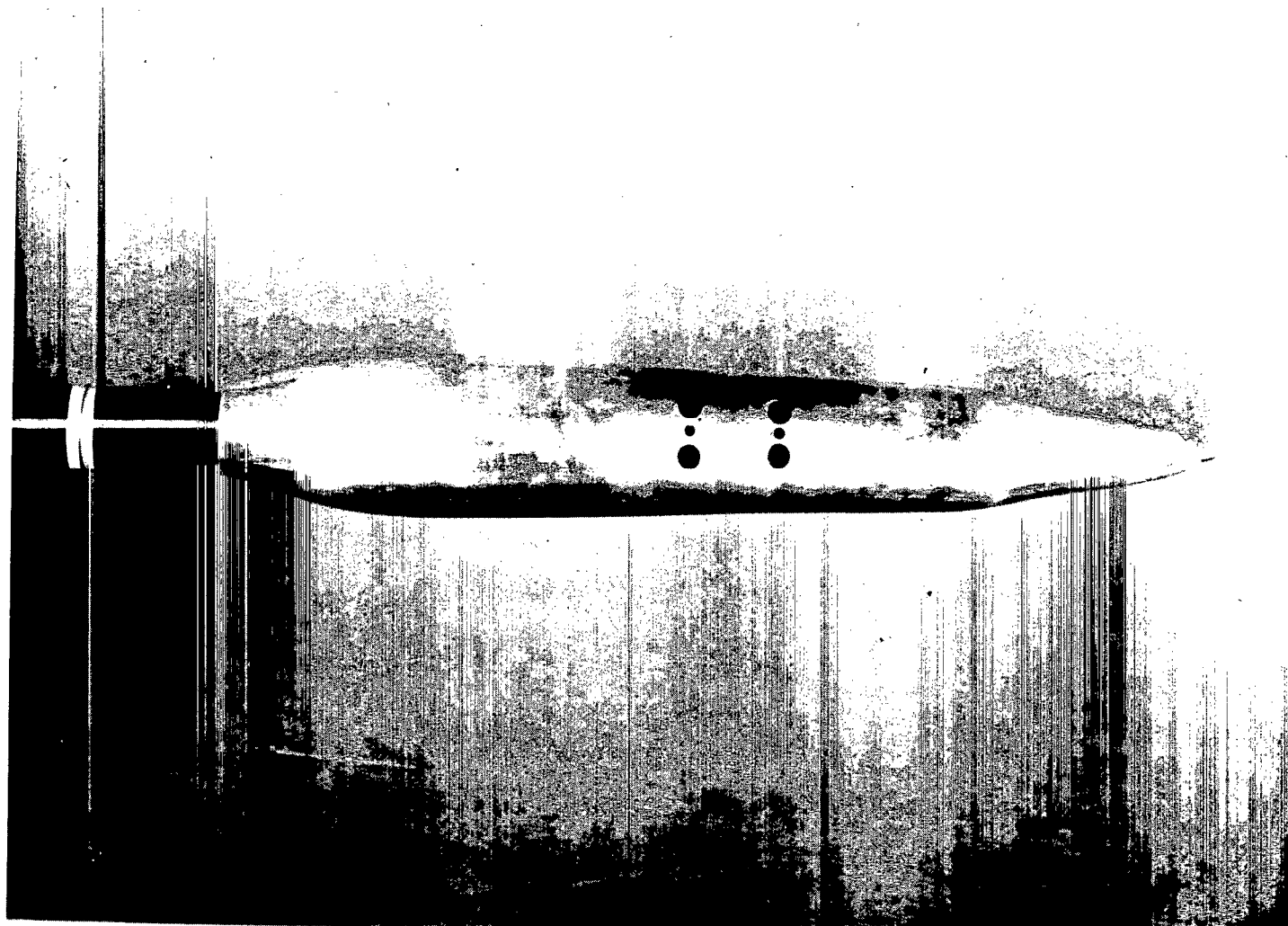


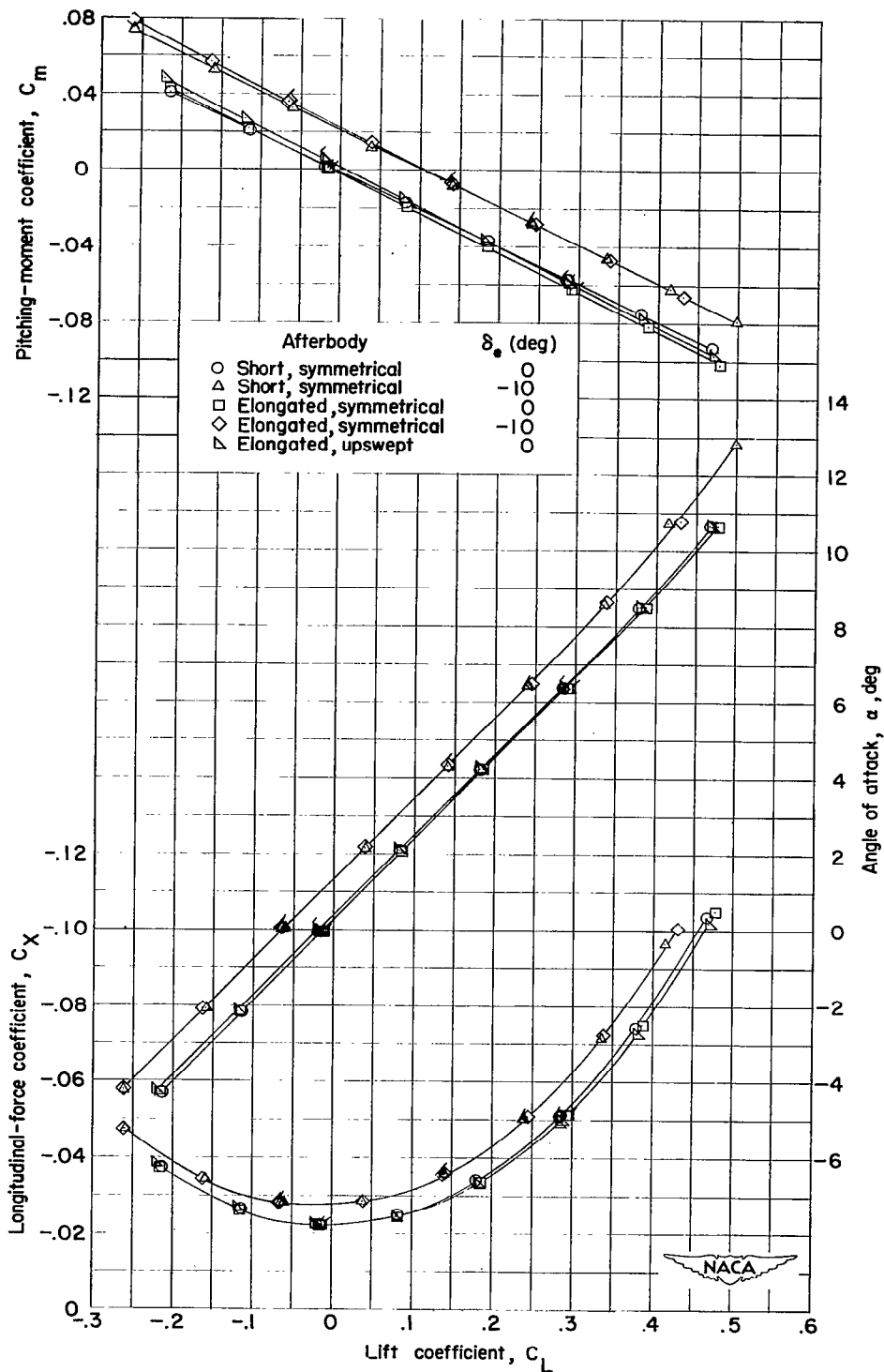
Figure 5.- Area distribution for complete configuration with different afterbodies.



CONFIDENTIAL

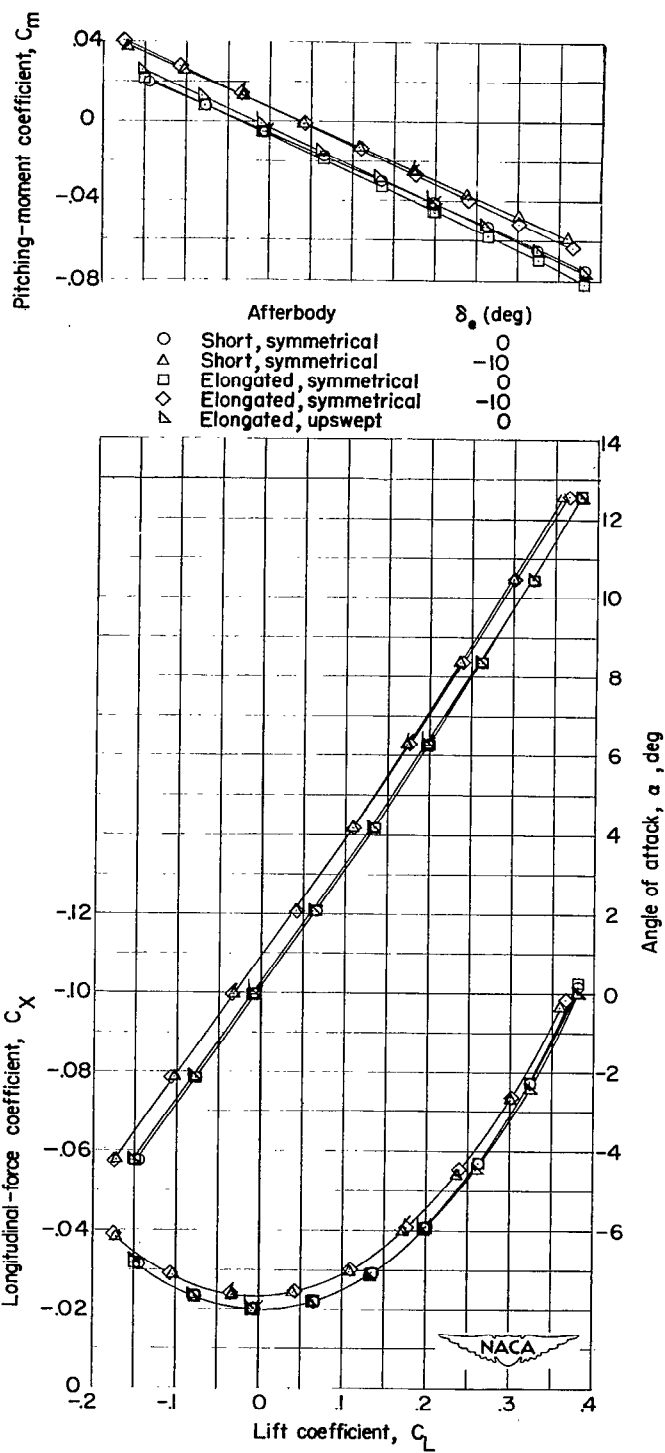
L-78239

Figure 6.- Photograph of the Convair MX-1554 "equivalent-area" body of revolution.



(a) $M = 1.41$; $R = 4.8 \times 10^6$.

Figure 7.- Aerodynamic characteristics in pitch of the Convair MX-1554 model with different afterbodies.



(b) $M = 2.01$; $R = 3.96 \times 10^6$.

Figure 7.- Concluded.

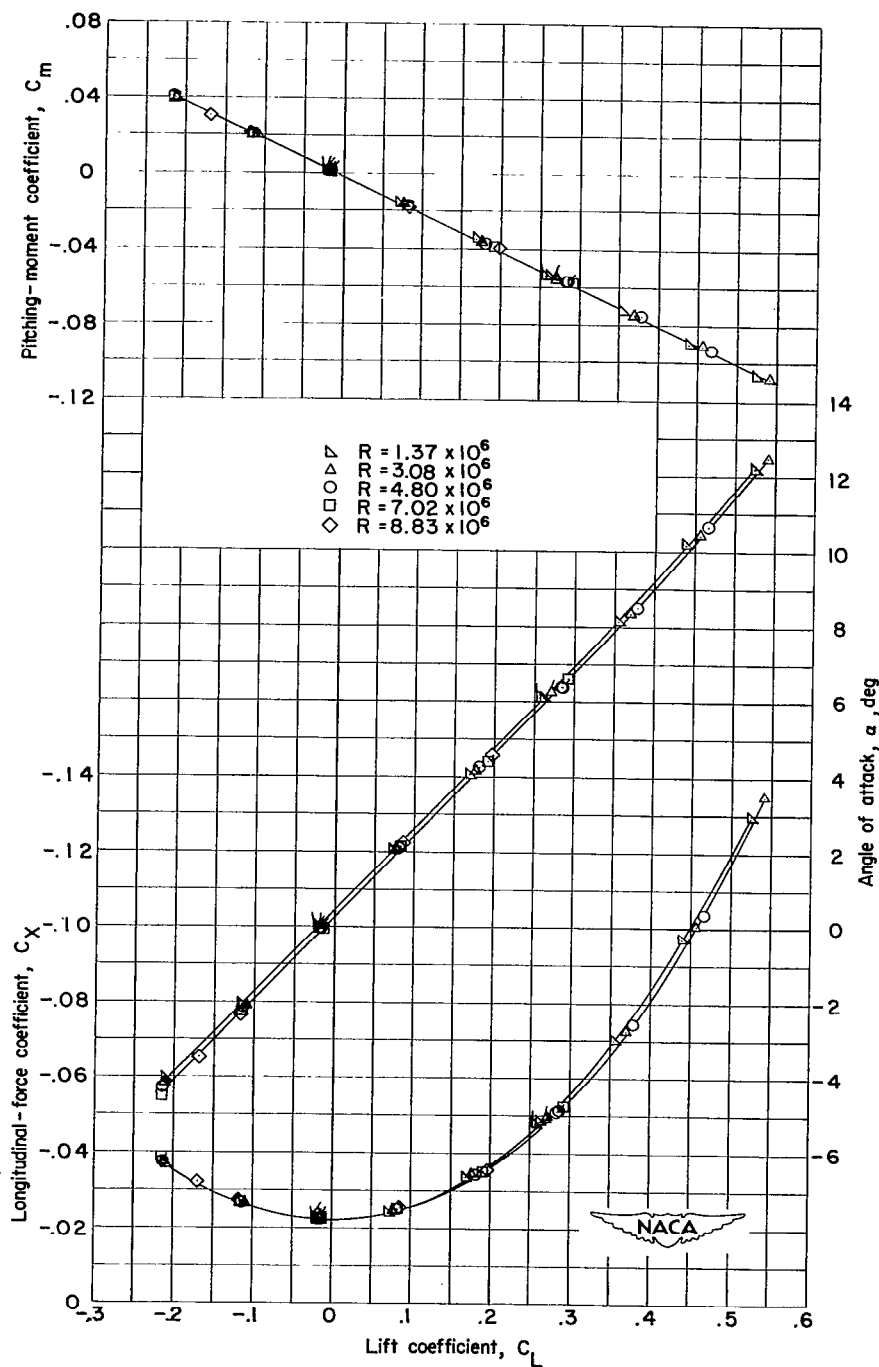
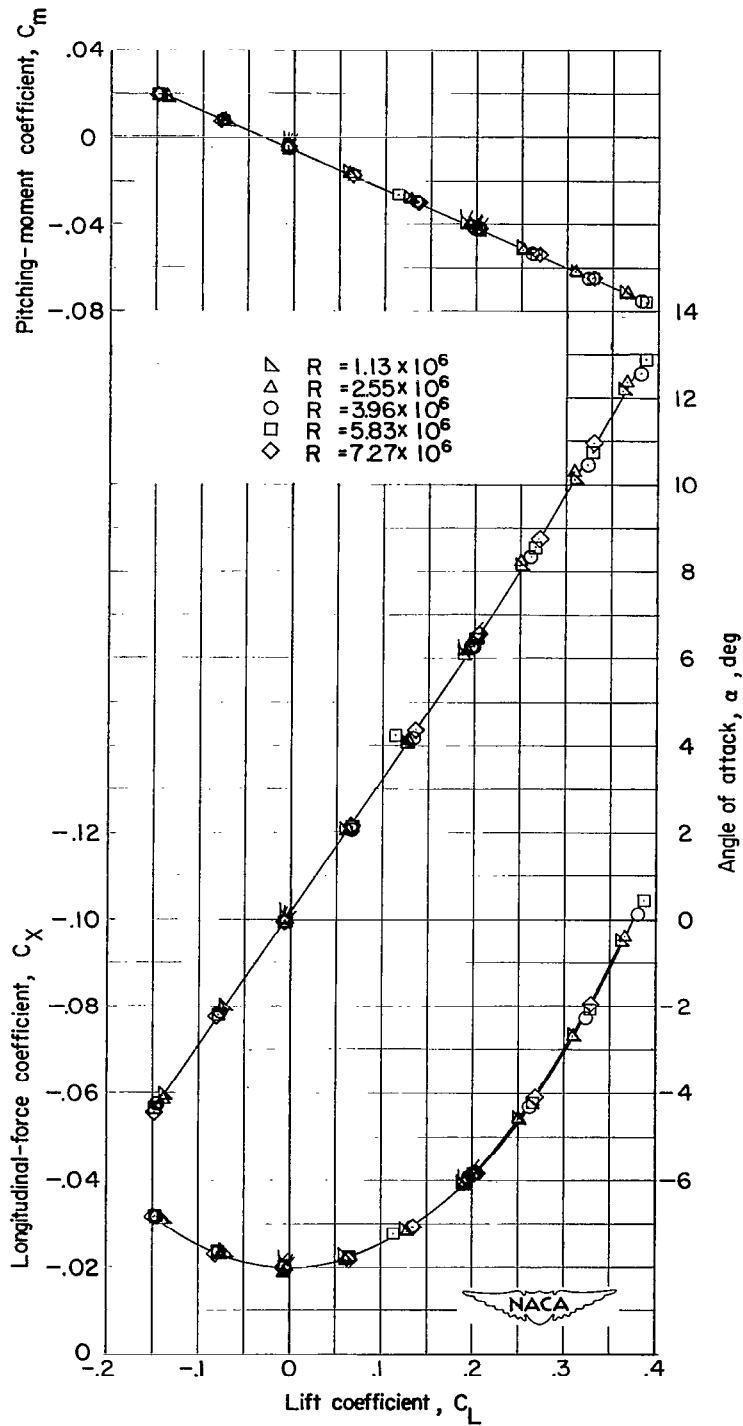
(a) $M = 1.41$.

Figure 8.- Effect of Reynolds number on the aerodynamic characteristics of the basic configuration (short symmetrical afterbody) of the Convair MX-1554 model in pitch.



(b) $M = 2.01$.

Figure 8.- Concluded.

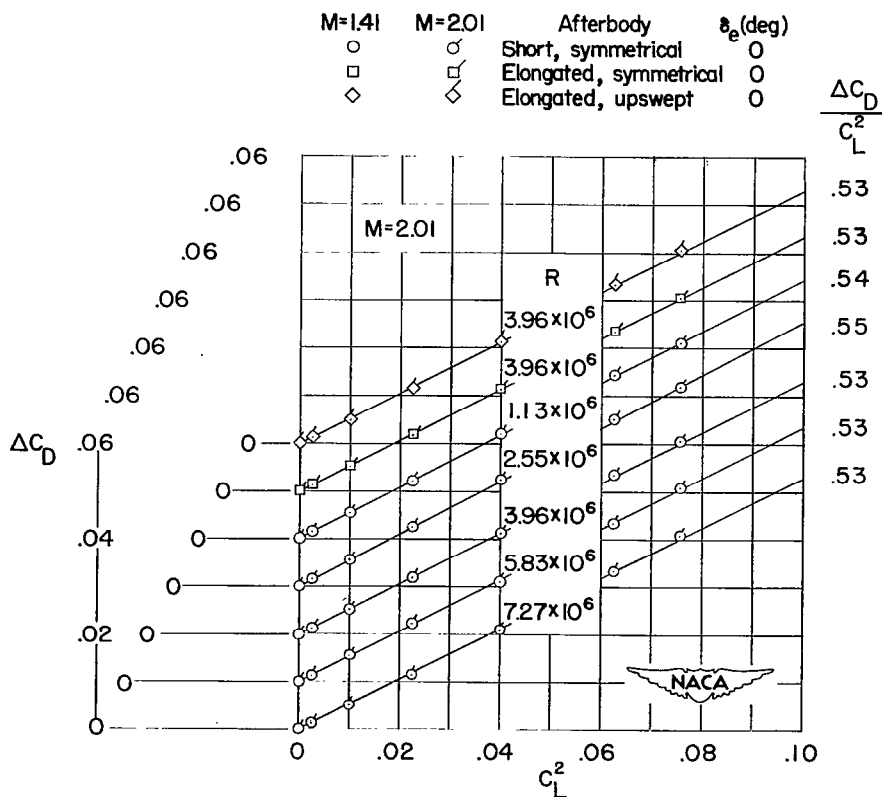
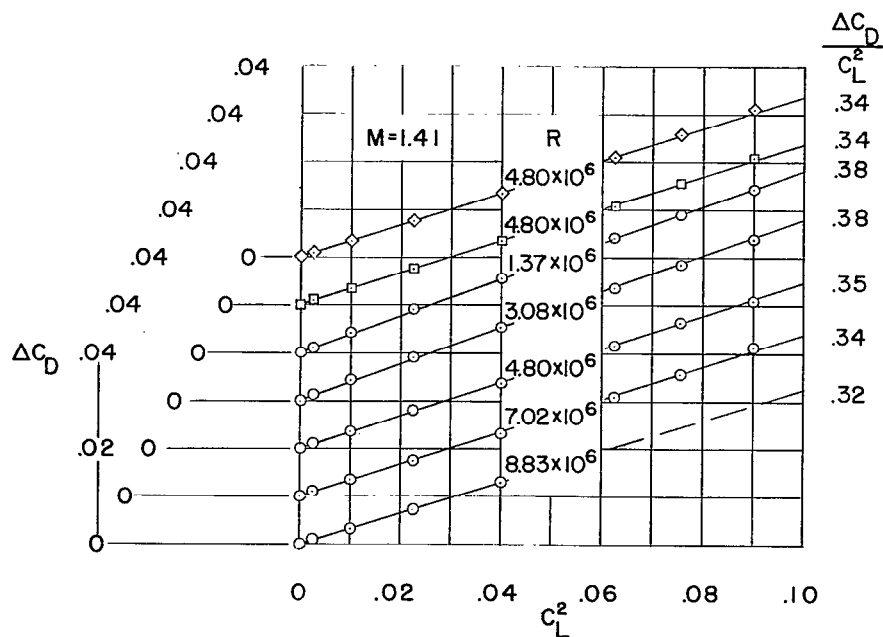


Figure 9.- Drag due to lift of the various test configurations at $M = 1.41$ and 2.01 . R = variable.

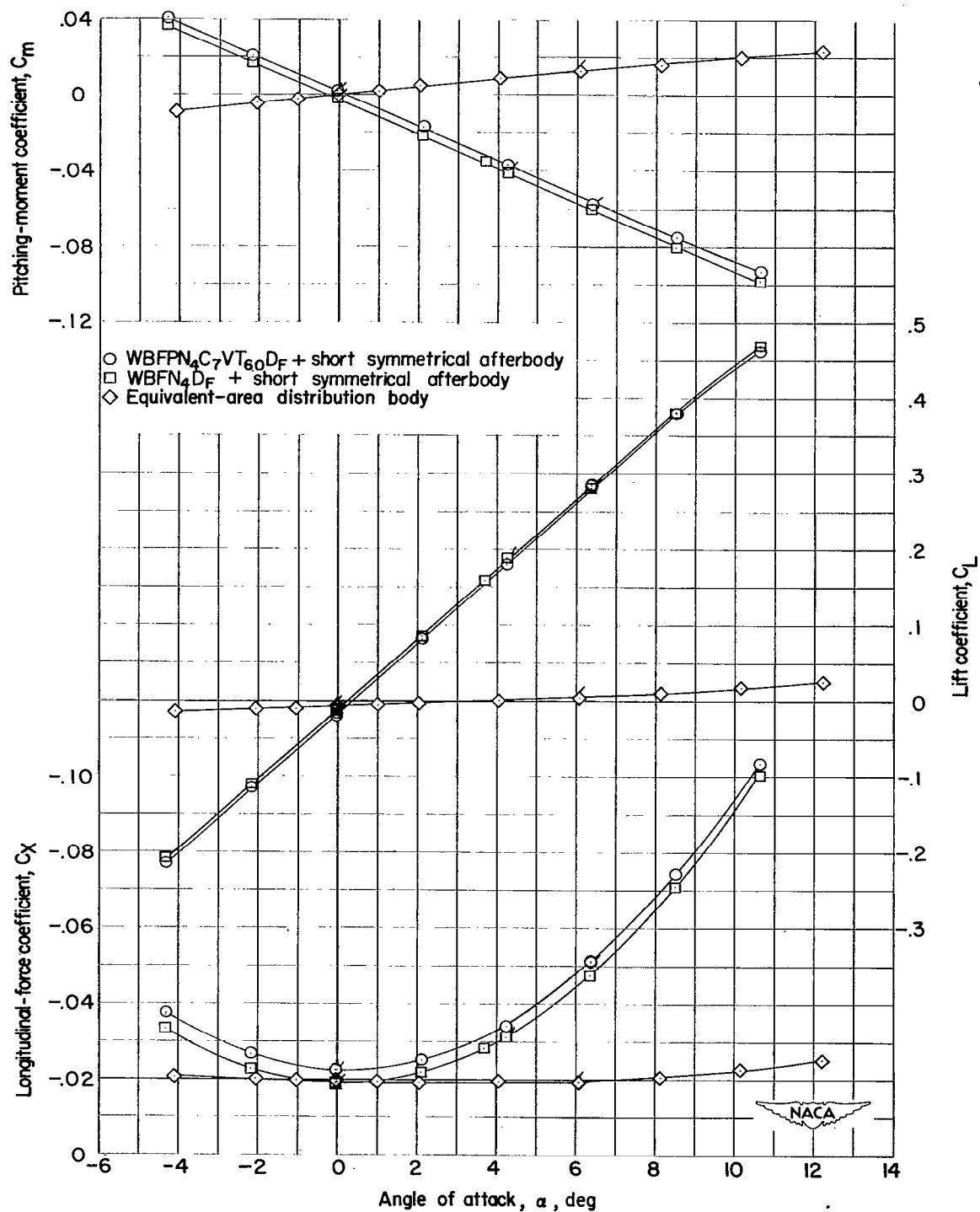
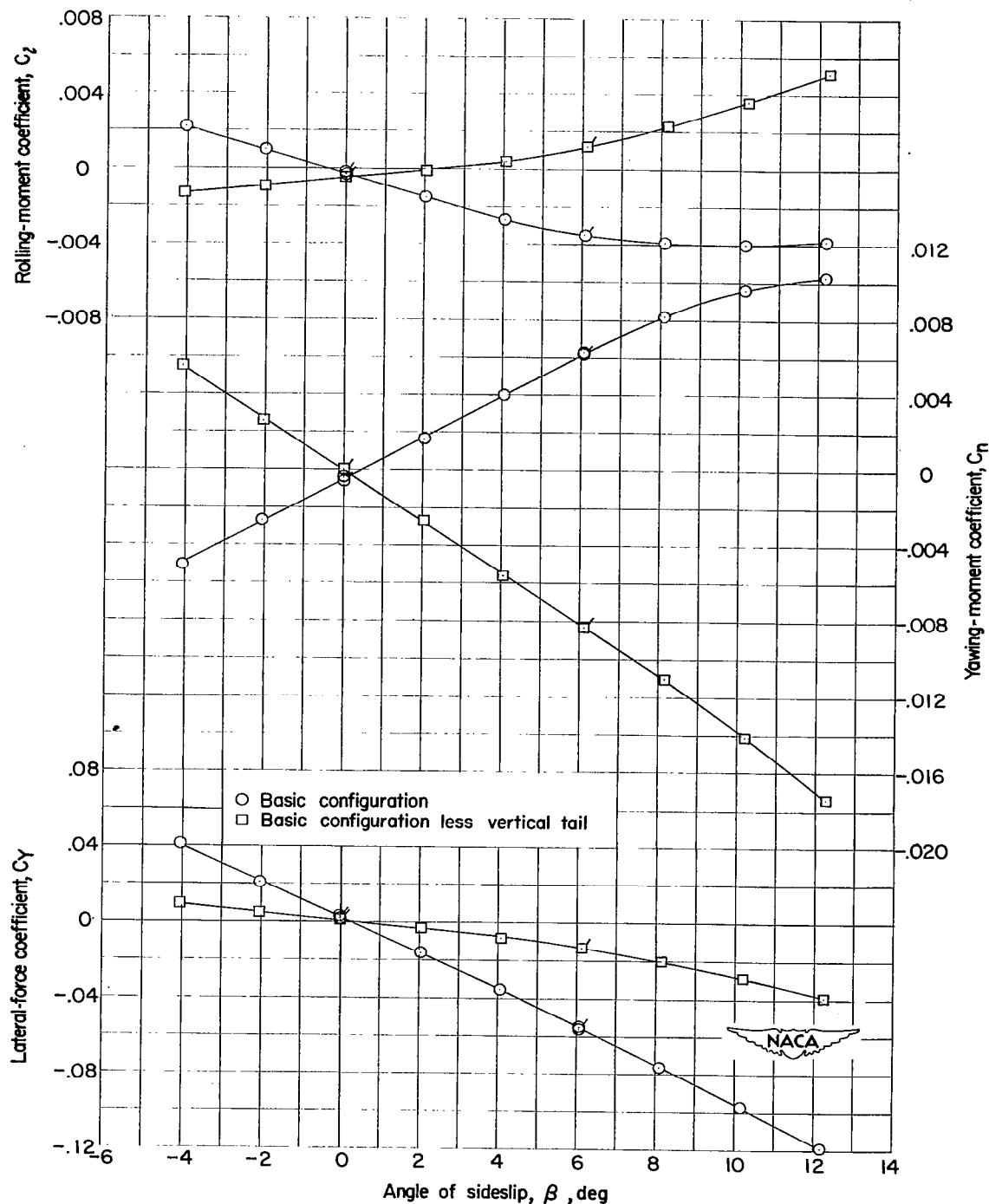
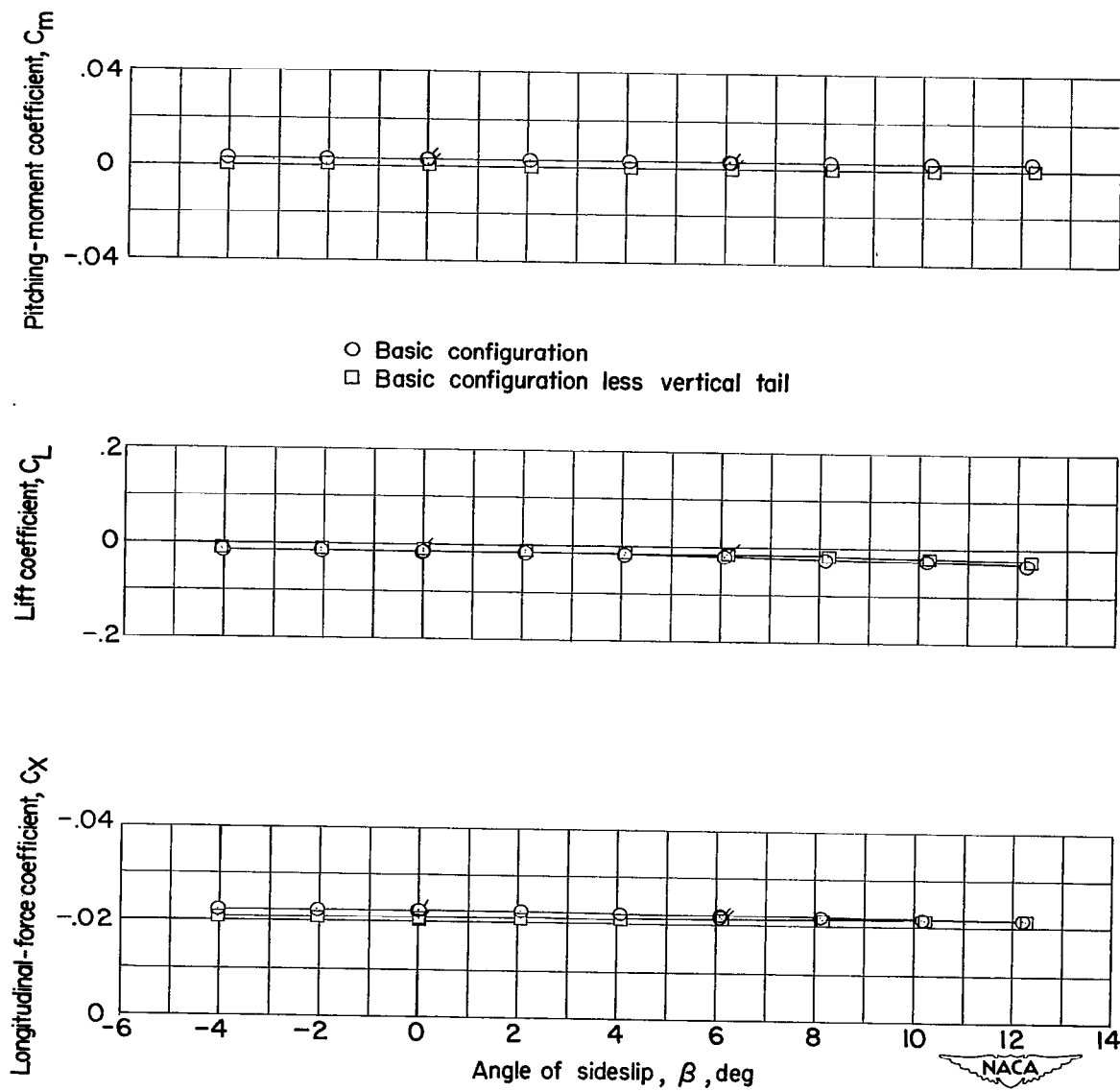


Figure 10.- Aerodynamic characteristics in pitch for the MX-1554 and the equivalent-area distribution body of the Convair MX-1554. $M = 1.41$; $R = 4.8 \times 10^6$.



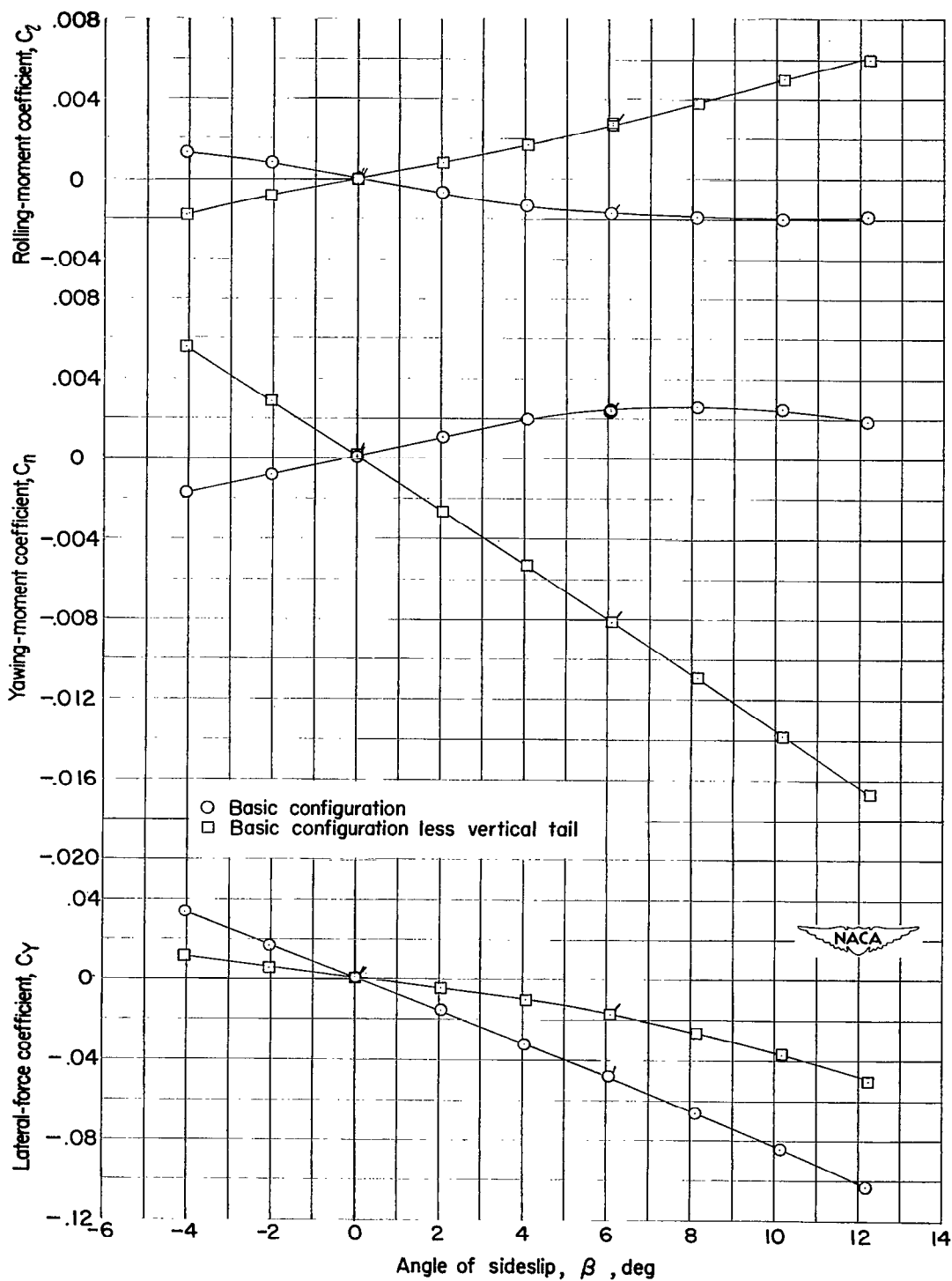
(a) $M = 1.41$; $R = 4.8 \times 10^6$.

Figure 11.- Aerodynamic characteristics of the basic configuration (short symmetrical afterbody) of the Convair MX-1554 model in sideslip, with and without vertical tail. $\alpha = 0^\circ$.



(a) Concluded. $M = 1.41$; $R = 4.8 \times 10^6$.

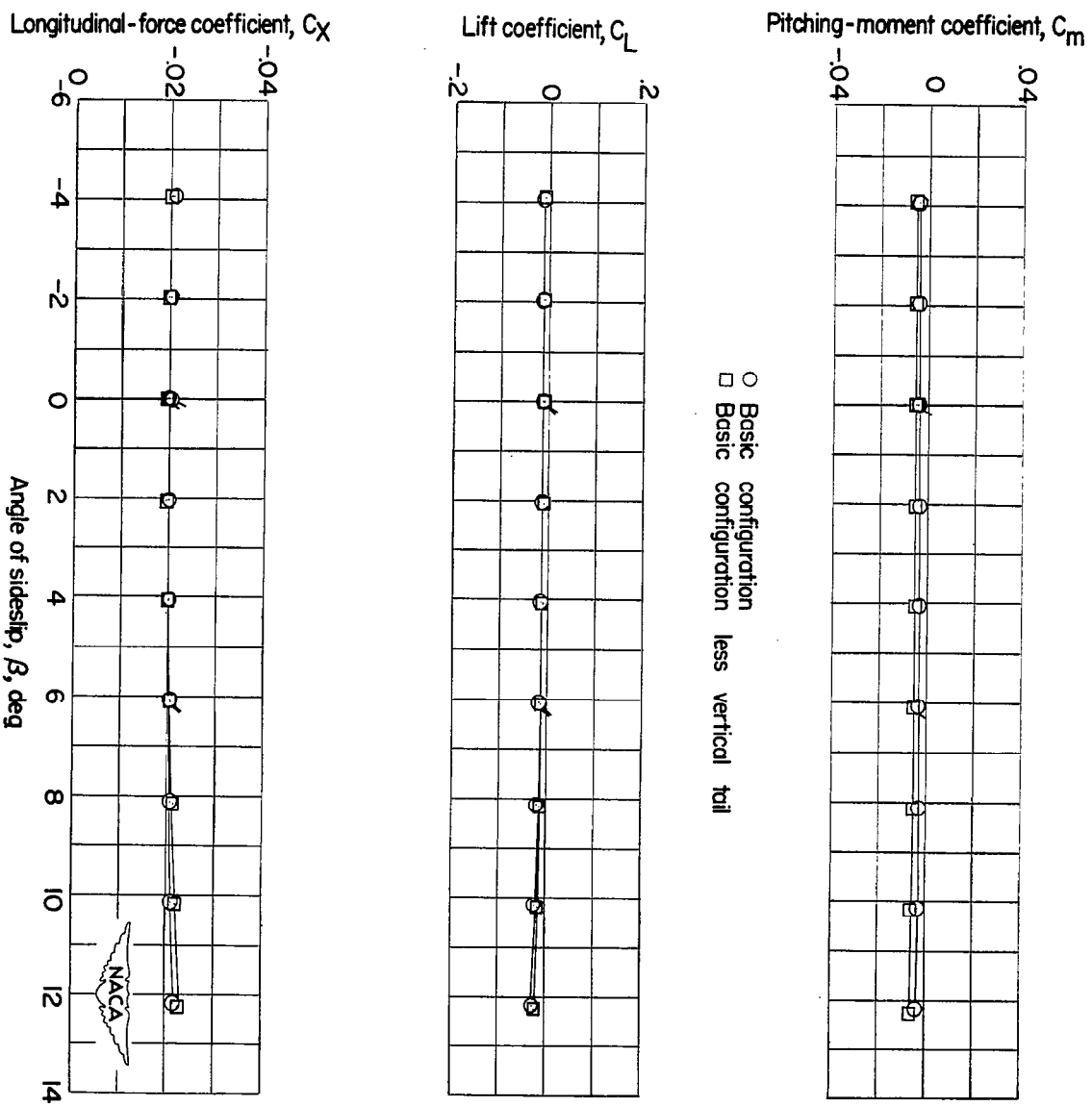
Figure 11.- Continued.



(b) $M = 2.01$; $R = 3.96 \times 10^6$.

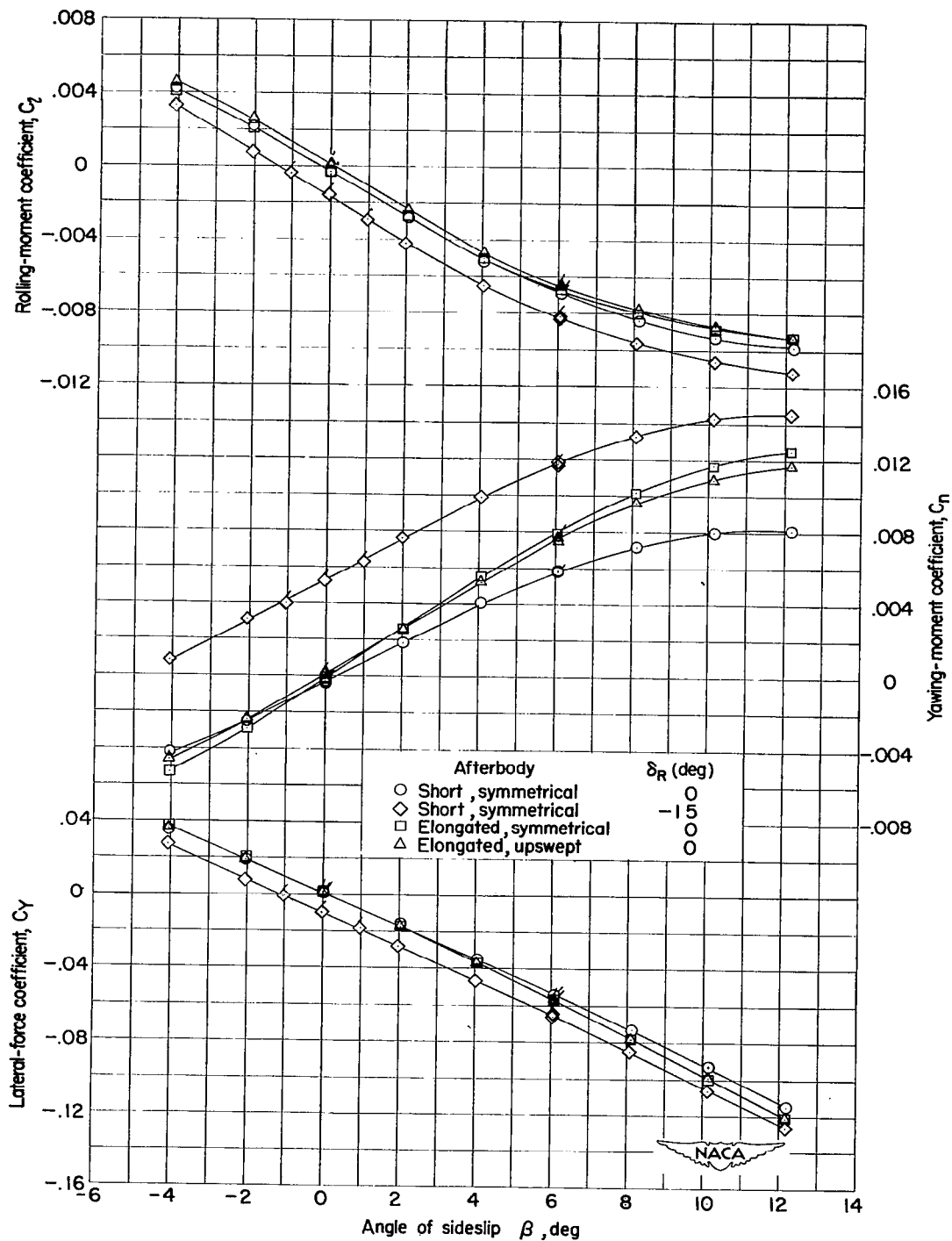
Figure 11.- Continued.

11
12
13
14
15
16
17
18
19
20
21
22
23
24
25
26
27
28
29
30
31
32
33
34
35
36
37
38
39
40
41
42
43
44
45
46
47
48
49
50
51
52
53
54
55
56
57
58
59
60
61
62
63
64
65
66
67
68
69
70
71
72
73
74
75
76
77
78
79
80
81
82
83
84
85
86
87
88
89
90
91
92
93
94
95
96
97
98
99
100



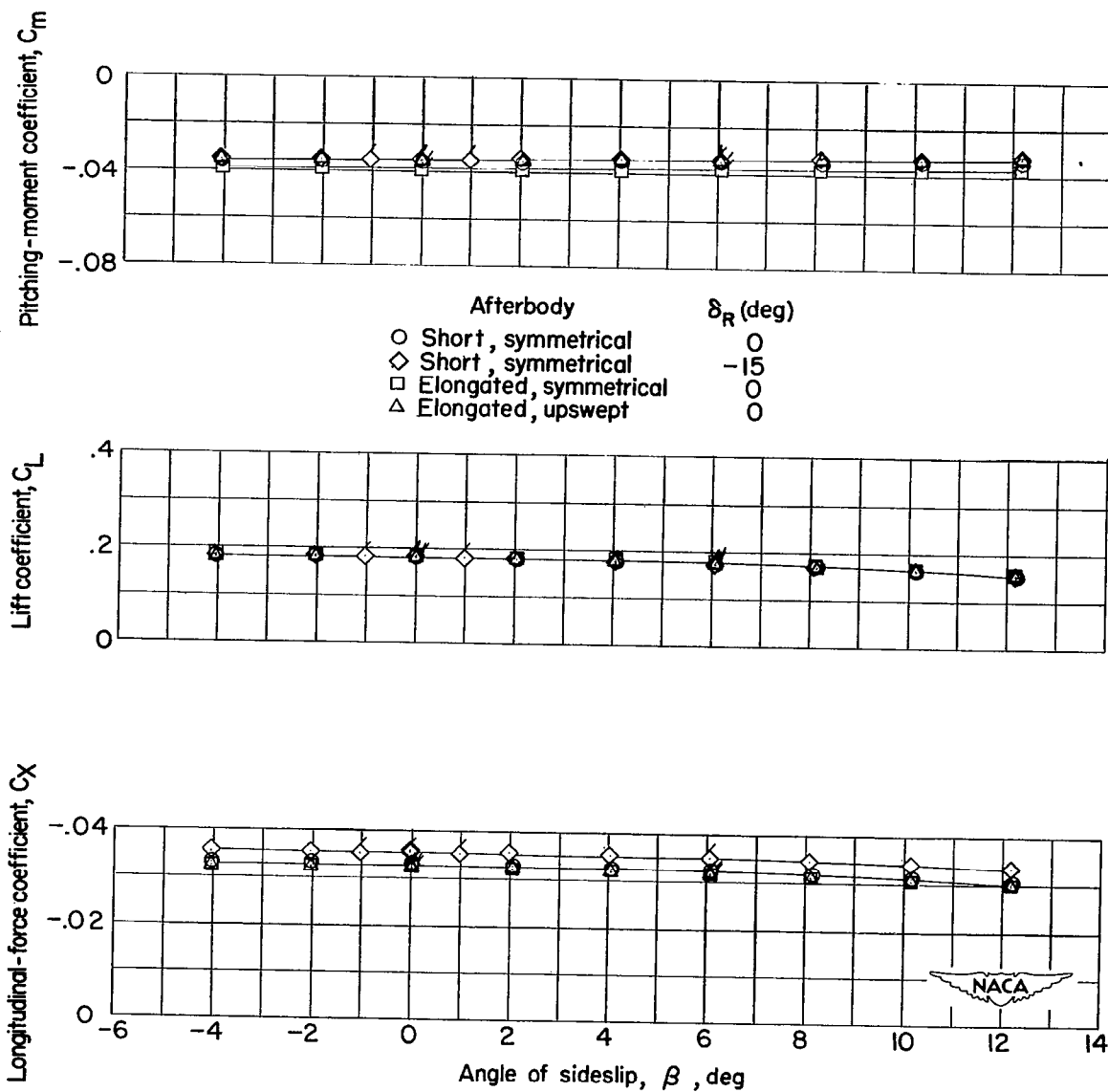
(b) Concluded. $M = 2.01$; $R = 3.96 \times 10^6$.
 Figure 11.- Concluded.

CONFIDENTIAL



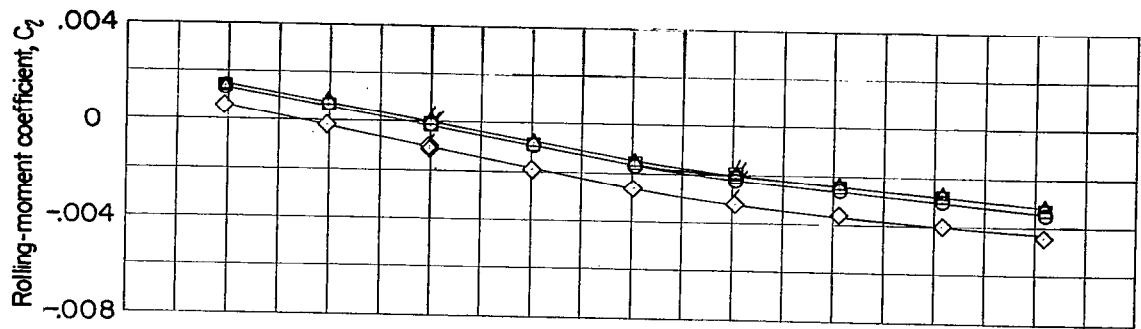
(a) $M = 1.41$; $R = 4.8 \times 10^6$.

Figure 12.- Aerodynamic characteristics of the Convair MX-1554 model in sideslip with different afterbodies. $\alpha = 4^\circ$.



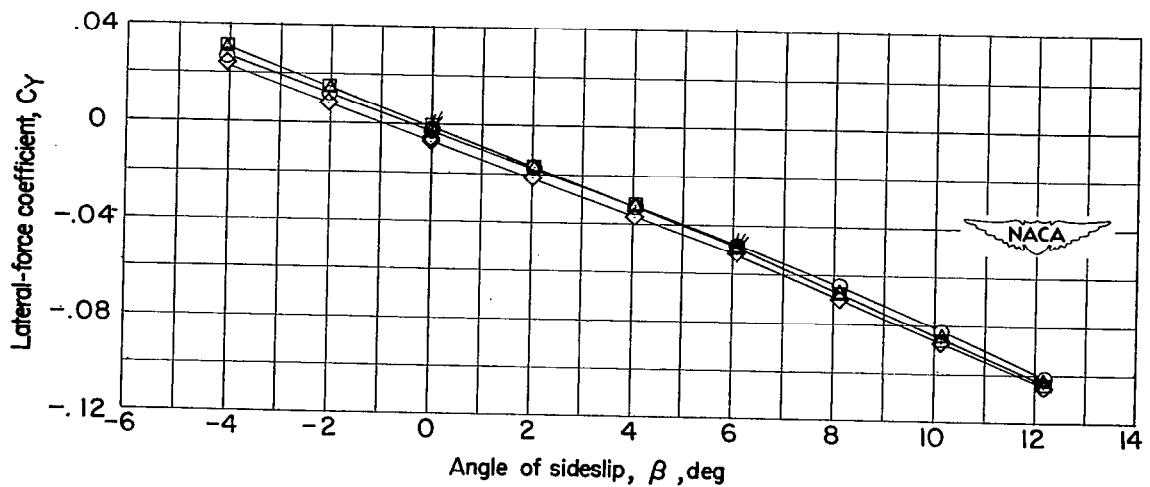
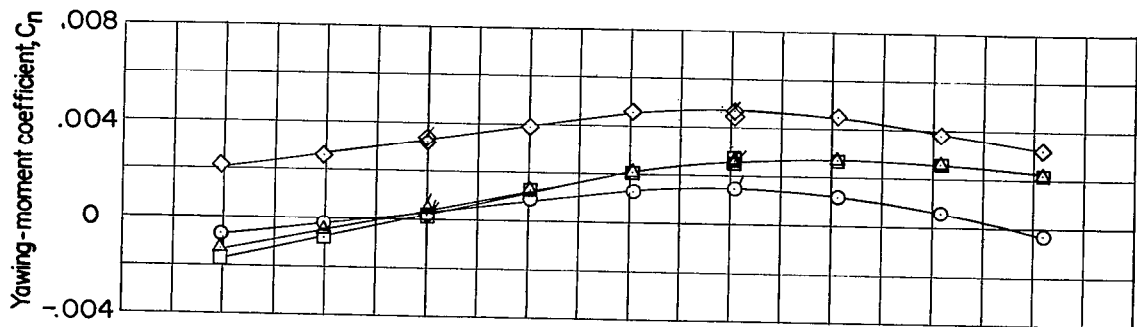
(a) Concluded. $M = 1.41$; $R = 4.8 \times 10^6$.

Figure 12.- Continued.



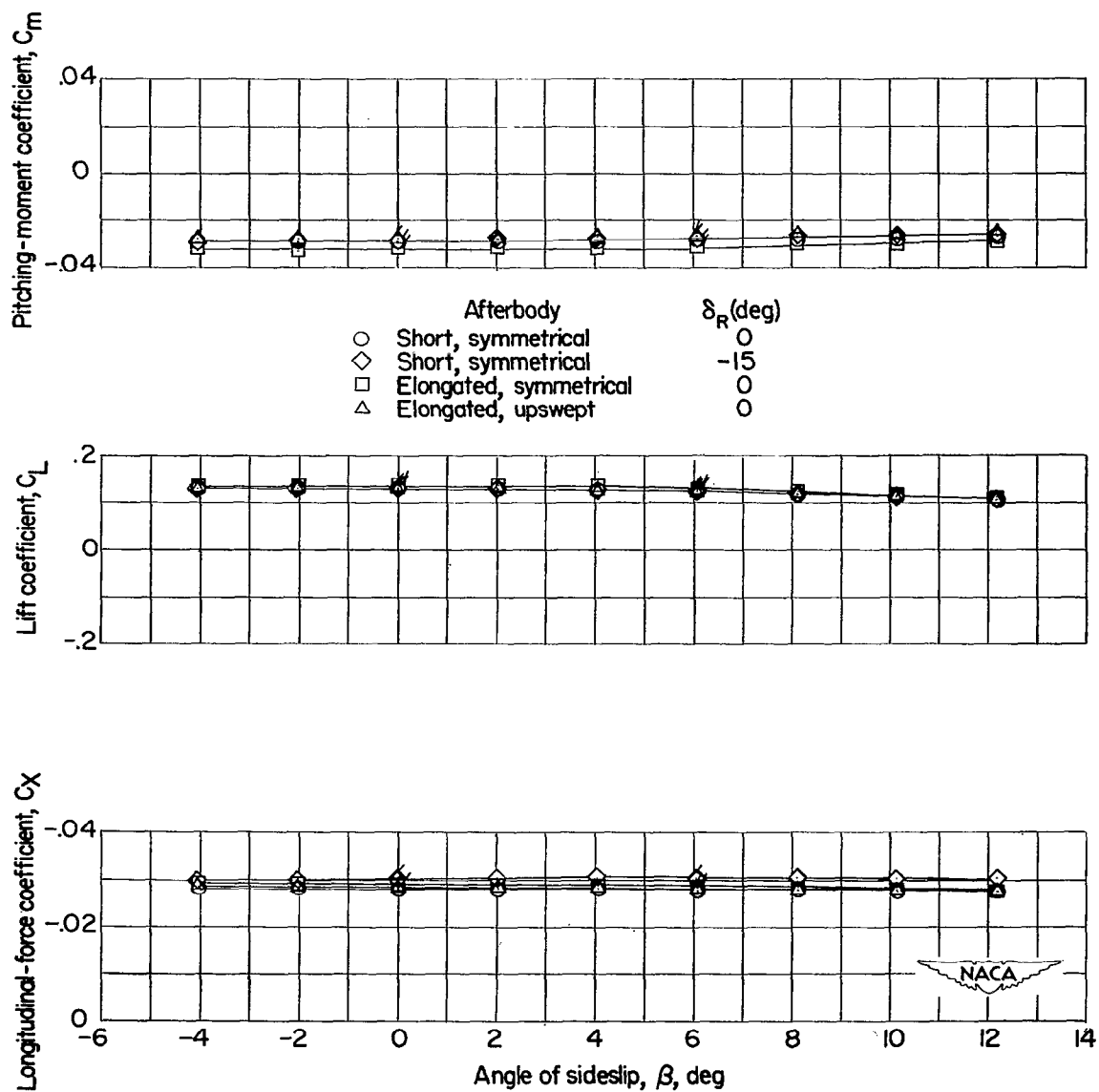
Afterbody δ_R (deg)

○ Short, symmetrical	0
◇ Short, symmetrical	-15
□ Elongated, symmetrical	0
△ Elongated, upswept	0



(b) $M = 2.01$; $R = 3.96 \times 10^6$.

Figure 12.- Continued.



(b) Concluded. $M = 2.01$; $R = 3.96 \times 10^6$.

Figure 12.- Concluded.

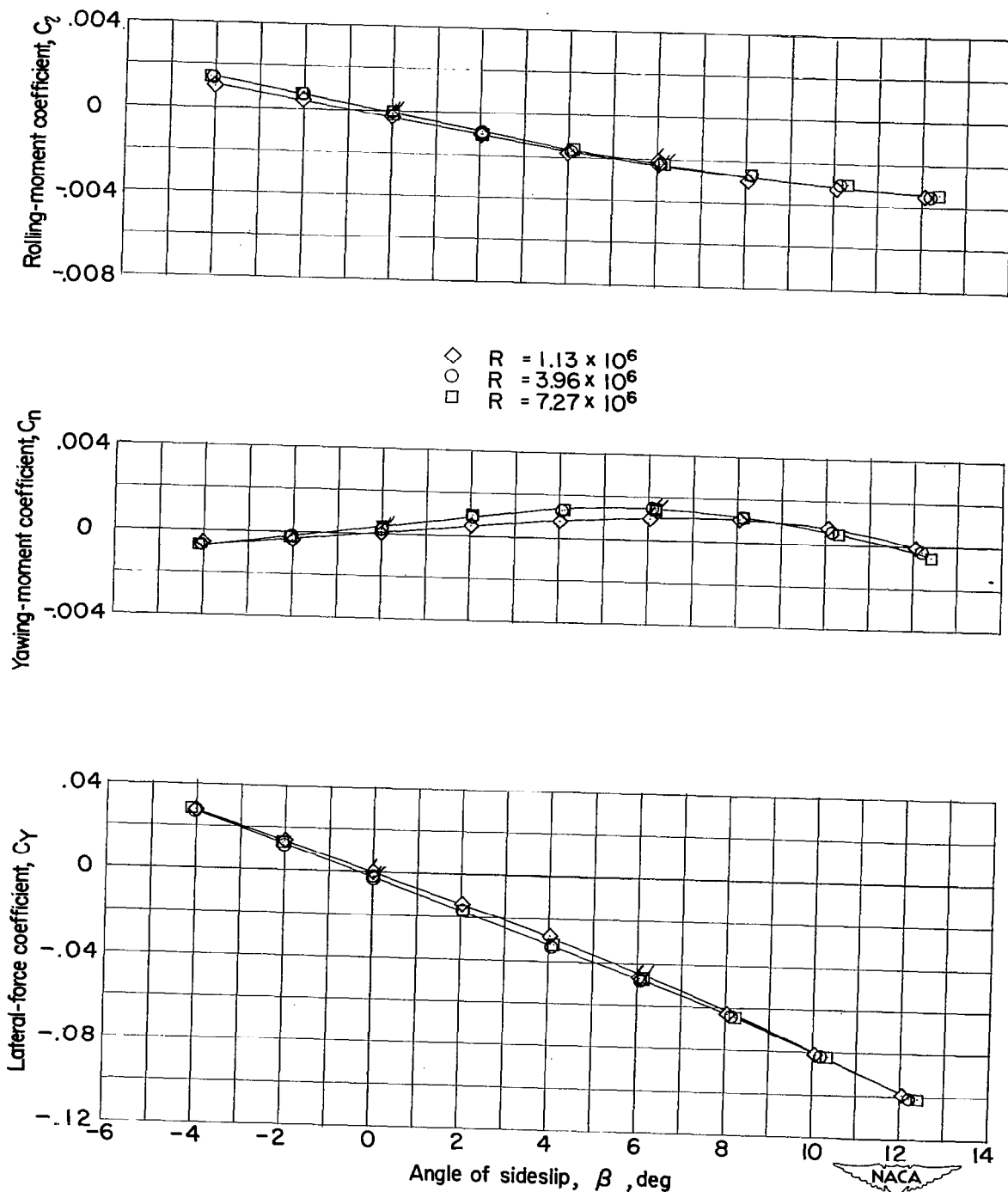


Figure 13.- Effect of Reynolds number on the aerodynamic characteristics of the basic configuration (short symmetrical afterbody) of the Convair MX-1554 model in sideslip. $\alpha = 4^\circ$; $M = 2.01$.

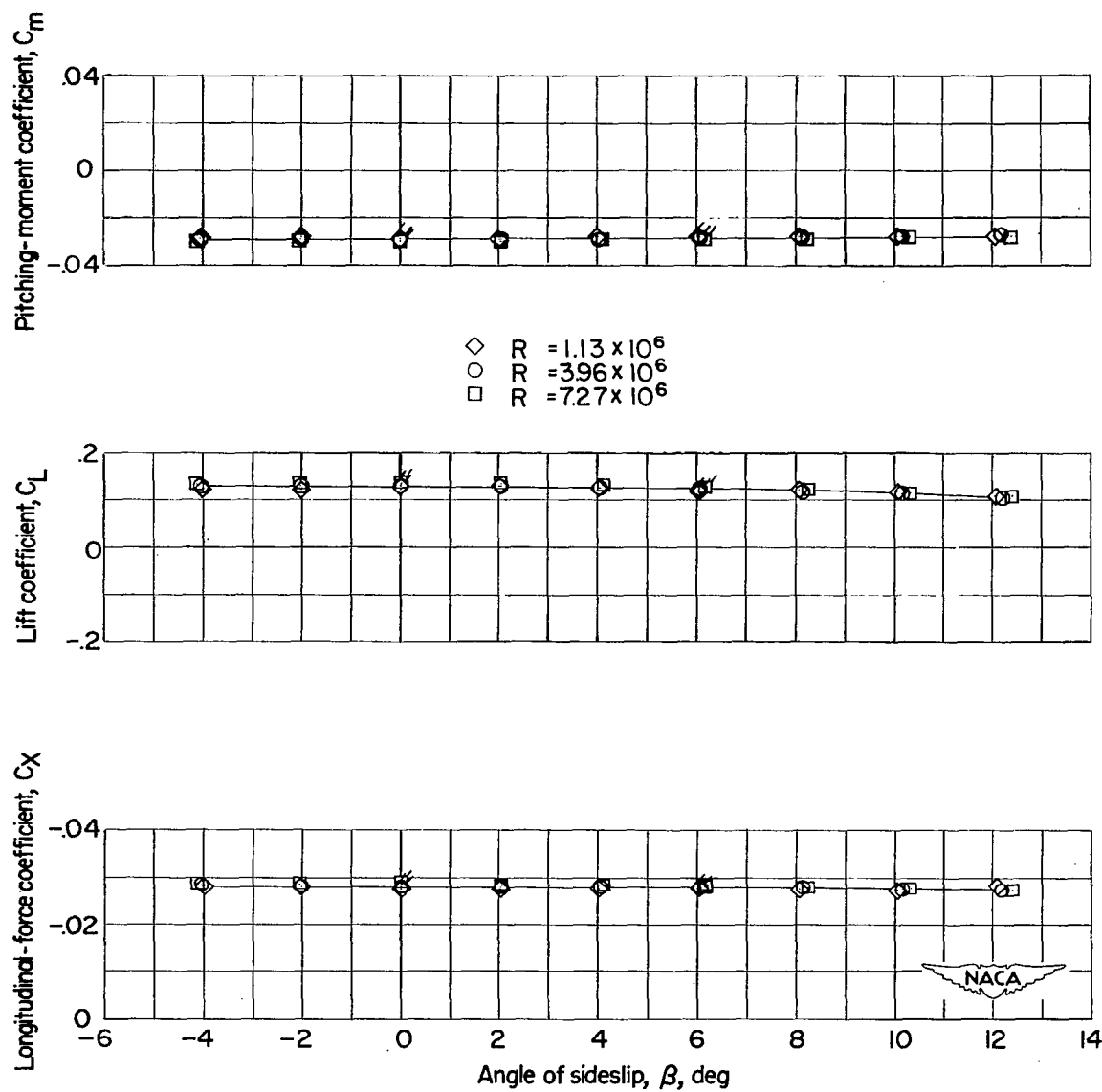


Figure 13.- Concluded.

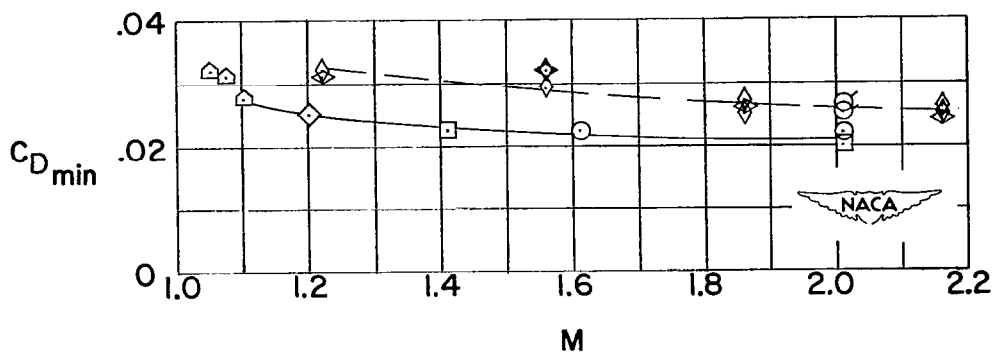
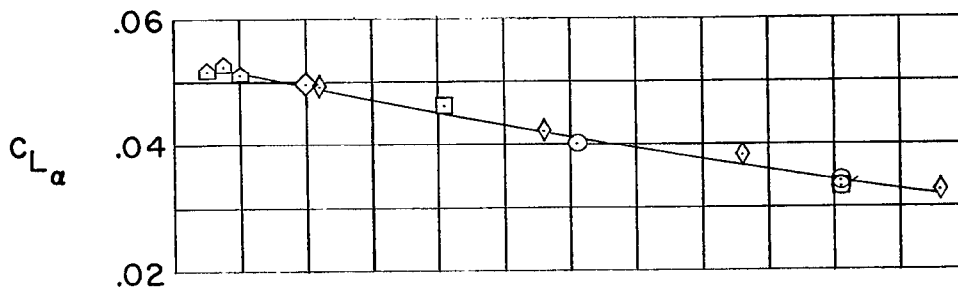
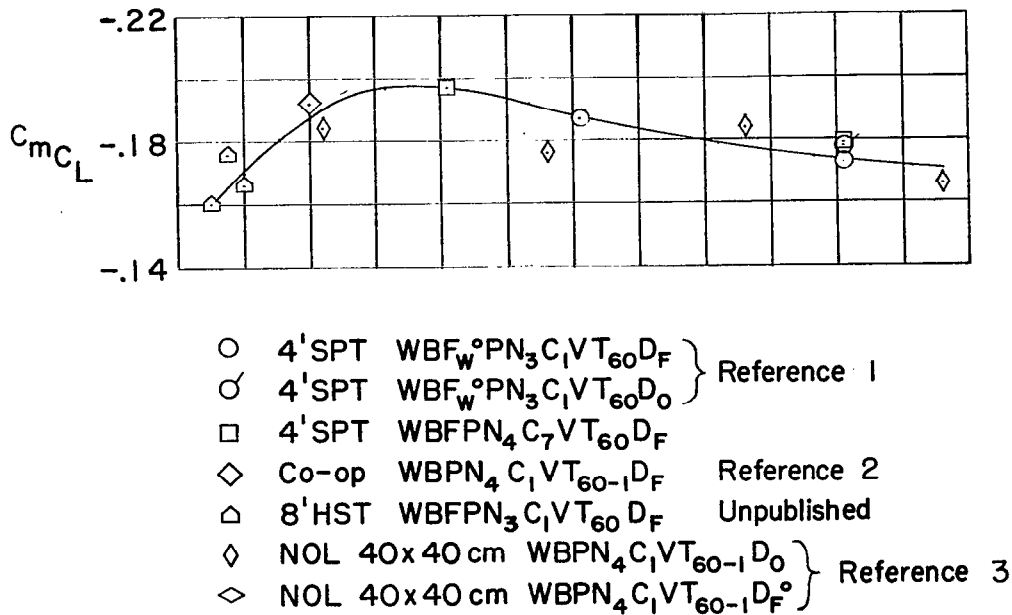
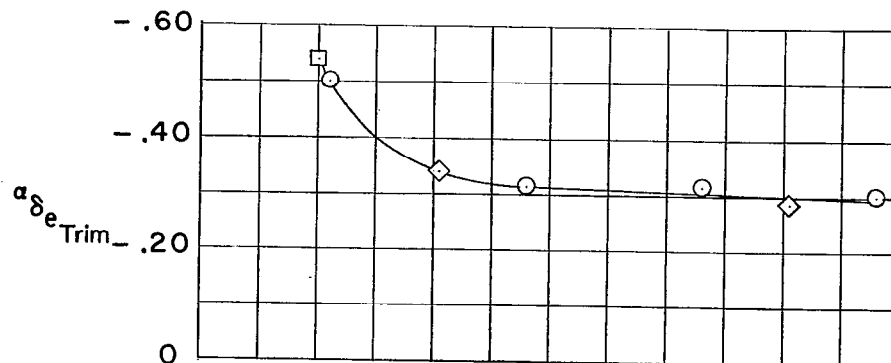
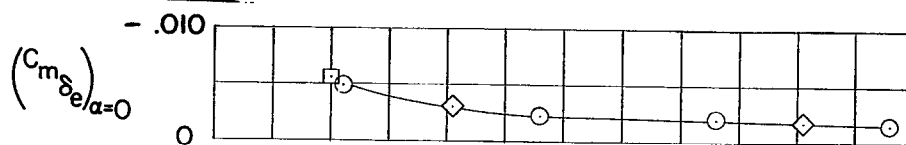


Figure 14.- Longitudinal parameters of the Convair MX-1554 through the supersonic Mach number range. $\beta = 0^\circ$.



- ◇ 4'SPT WBFPN₄C₇VT₆₀D_F
- Co-op WBPN₄C₁VT₆₀₋₁D_F Reference 2
- NOL 40 x 40 cm WBPN₄C₁VT₆₀₋₁D₀ Reference 3

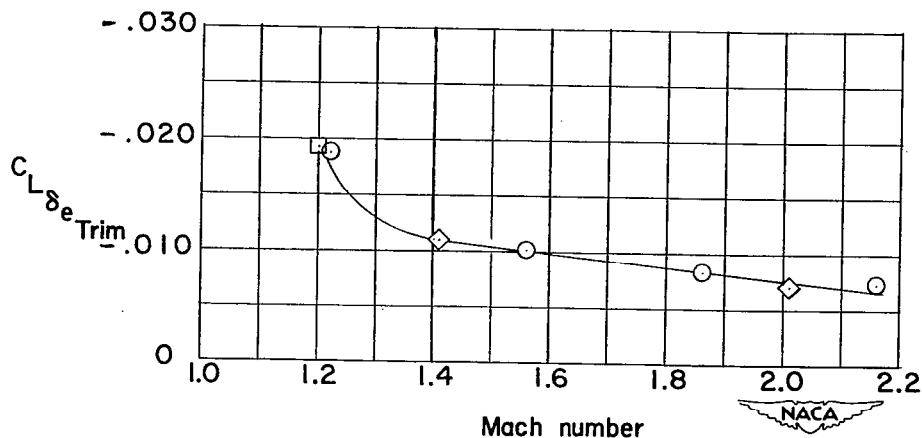
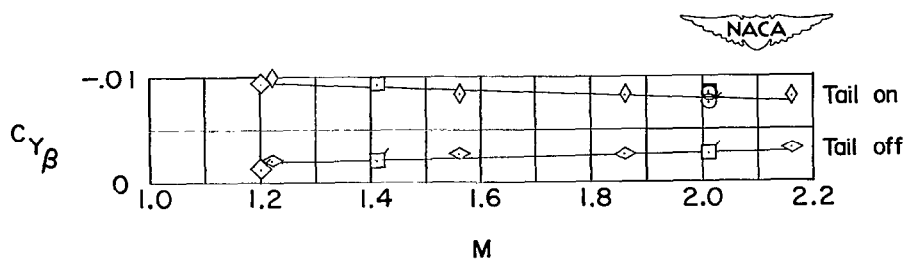
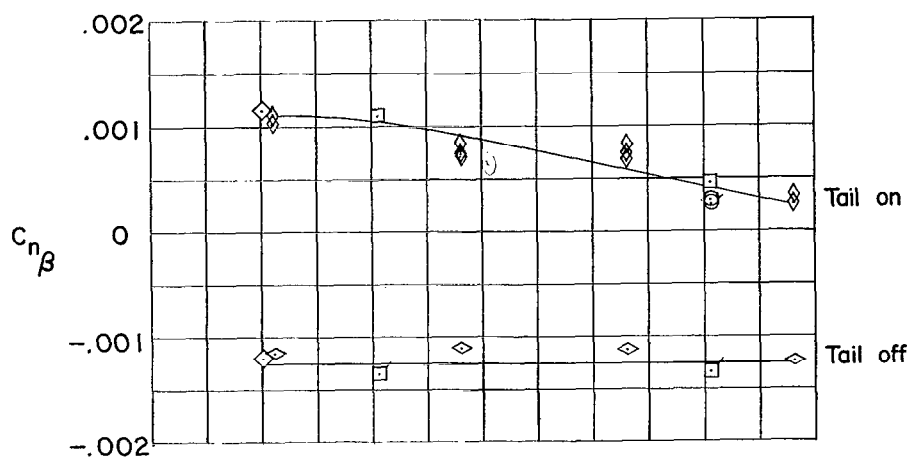
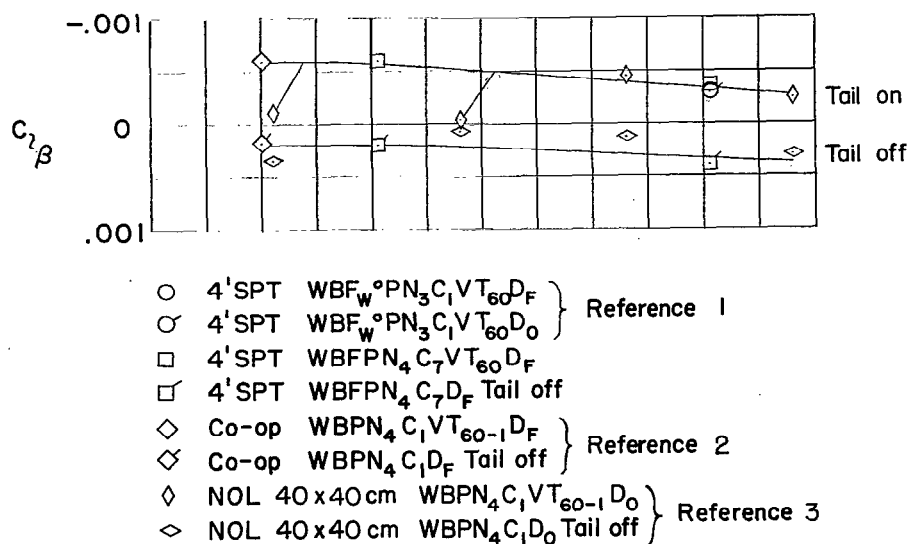
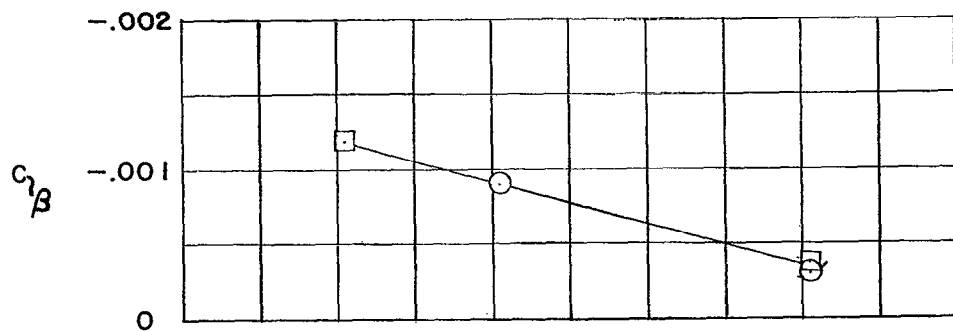


Figure 15.- Longitudinal control parameters of the Convair MX-1554 model through the supersonic Mach number range.

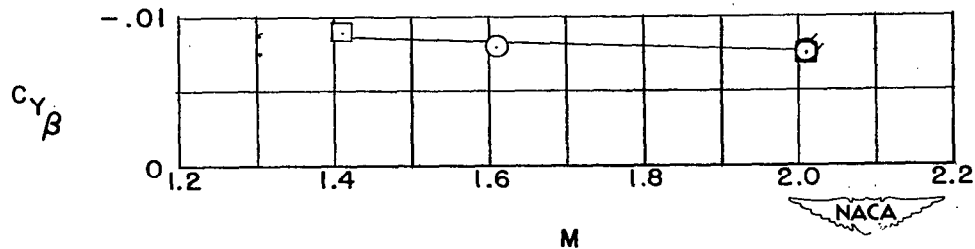
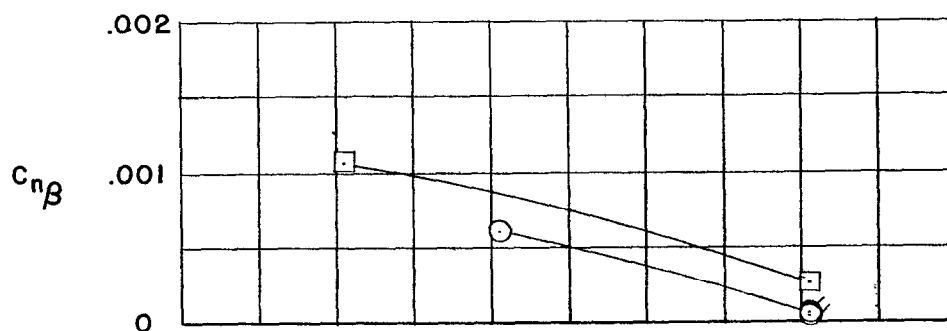


(a) $\alpha = 0^\circ$.

Figure 16.- Lateral parameters of the Convair MX-1554 model through the supersonic Mach number range.



- \bigcirc 4'SPT WBF_w^oPN₃C₁VT₆₀D_F } Reference 1
 \bigcirc 4'SPT WBF_w^oPN₃C₁VT₆₀D₀ }
 \square 4'SPT WBF PN₄C₇VT₆₀D_F



(b) $\alpha = 4^\circ$.

Figure 16.- Concluded.

CONFIDENTIAL

SECURITY INFORMATION

NASA Technical Library



L

3 1176 01438 6081

CONFIDENTIAL